Crosstalk and signalling switches in mitogen-activated protein kinase cascades

Dirk Fey[1], David R Croucher[1], Walter Kolch[1], Boris N Kholodenko[1,*]

Abstract

Mitogen-activated protein kinase (MAPK) cascades control cell fate decisions, such as proliferation, differentiation and apoptosis by integrating and processing intra- and extracellular cues. However, similar MAPK kinetic profiles can be associated with opposing cellular decisions depending on cell type, signal strength and dynamics. This implies that signalling by each individual MAPK cascade has to be considered in the context of the entire MAPK network. Here, we develop a dynamic model of feedback and crosstalk for the three major MAPK cascades; extracellular signal-regulated kinase (ERK), p38 mitogen-activated protein kinase (p38), c-Jun N-terminal kinase (JNK), and also include input from protein kinase B (AKT) signalling. Focusing on the bistable activation characteristics of the JNK pathway, this model explains how pathway crosstalk harmonises different MAPK responses resulting in pivotal cell fate decisions. We show that JNK can switch from a transient to sustained activity due to multiple positive feedback loops. Once activated, positive feedback locks JNK in a highly active state and promotes cell death. The switch is modulated by the ERK, p38 and AKT pathways. ERK activation enhances the dual specificity phosphatase (DUSP) mediated dephosphorylation of JNK and shifts the threshold of the apoptotic switch to higher inputs. Activation of p38 restores the threshold by inhibiting ERK activity via the PP1 or PP2A phosphatases. Finally, AKT activation inhibits the JNK positive feedback, thus abrogating the apoptotic switch and allowing only proliferative signalling. Our model facilitates understanding of how cancerous deregulations disturb MAPK signal processing and provides explanations for certain drug resistances. We highlight a critical role of DUSP1 and DUSP2 expression patterns in facilitating the switching of JNK activity and show how oncogene induced ERK hyperactivity prevents the normal apoptotic switch explaining the failure of certain drugs to induce apoptosis.

Manuscript length:
11 pages (not counting figures, tables, abstract and references),
7263 words + 105 inline equations + 14 display equations (by http://app.uio.no/ifi/texcount/),
9 figures,
5 tables.

[1] Systems Biology Ireland, University College Dublin, Ireland

[*]Correspondence:
Boris N Kholodenko
Systems Biology Ireland
Conway Institute
University College Dublin
Belfield
Dublin 4
boris.kholodenko@ucd.ie

1 Introduction

A hallmark of cancer is dysregulation of pivotal cell fate decisions leading to aberrant proliferation and reduced apoptosis (Hanahan and Weinberg, 2011). Healthy cell fate decisions depend on a proper sensing of the cell's intra- and extracellular environment in a process called signal transduction (Kholodenko et al., 2010). The signals are sensed by receptors that bind their cognate extracellular ligands, resulting in conformational changes that trigger the formation of multi-protein complexes and subsequent activation of GTPases and kinases (Lemmon and Schlessinger, 2010). Hereby, one receptor usually activates several downstream pathways. Main transducers are MAPK cascades, which consist of a linear array of three kinases where a GTPase activates a MAPK kinase kinase (MAPKKK; MAP3K), which phosphorylates and activates a MAPK kinase (MAPKK; MAP2K), which in turn activates a MAPK that delivers the main pathway output by phosphorylation of multiple substrates (Dhillon et al., 2007; Kolch, 2005). MAPKs and MAP2Ks are activated by dual phosphorylation, which can confer switch-like properties to the activation kinetics (Kholodenko, 2000). Sometimes a MAP4K is intercalated between the GTPase and the MAP3K. A particular cell fate cannot be attributed to the activity of a single protein in isolation, but rather depends on the context, including the temporal patterns of activation and the regulatory feedback structures within the signalling network (Kholodenko et al., 2010; Nakakuki et al., 2010; Kholodenko, 2006). Because of this complexity, the function of cellular signalling often eludes a naive intuitive understanding, thus calling for the use of mathematical modelling and analysis (Kitano, 2010; Ireton et al., 2009; Kitano, 2002). Whereas others approach the problem from a less mechanistic viewpoint using regression (Miller-Jensen et al., 2007) or Boolean and semi-logic models (Saez-Rodriguez et al., 2011, 2009), we focus on dynamic models using ordinary differential equations.

Dynamic modelling has played a key role in understanding how signalling via the ERK cascade regulates cell fate (Kholodenko et al., 2010; Sturm et al., 2010). A classic example is growth factor signalling in Rat Pheochromocytoma (PC12) cells, where treatment with epidermal growth factor (EGF) or nerve growth factor (NGF) activates the same signalling cascade (the RAF/MEK/ERK cascade) but has different effects on cell fate. EGF causes transient activation of ERK and proliferation due to negative feedback, whereas NGF causes sustained ERK activation and differentiation due to positive feedback (von Kriegsheim et al., 2009; Santos et al., 2007). Similarly, the stress activated MAPKs JNK and p38 mediate diverse cellular responses. For example, growth factor induced, transient activation of JNK promotes cell survival and proliferation, whereas stress induced, prolonged JNK activity promotes growth arrest and cell death (Ventura et al., 2006). However, the mechanistic details of how this switch is generated and the factors determining the shift from proliferative to apoptotic JNK signalling are poorly understood, and mathematical modelling and analysis is largely lacking for stress activated kinases (Wagner and Nebreda, 2009; Bagowski and Ferrell, 2001).

Here, we provide a dynamic model of feedback and crosstalk for the three major MAPKs (ERK, p38, JNK) and protein kinase B (AKT) signalling. The model incorporates mechanistic details of positive feedback from JNK to its own MAP3Ks and negative crosstalk from and to other pathways. Using mathematical analysis, the model is used to decipher how JNK switches from proliferative to apoptotic signalling and how that switch is regulated by pathway crosstalk.

2 Results

We present a dynamic model of multiple MAPK cascade interactions featuring a JNK positive feedback loop that generates a proliferative-apoptotic switch. Further, we present a detailed analysis of factors controlling the dynamic properties of the JNK switch, with a particular focus on feedback loops and crosstalk.

2.1 Nominal model of MAPK interactions

Although MAPK signalling cascades have been studied extensively, the connectivity of MAPK systems is not completely understood. MAPKs feature several isoforms, a high number of inputs in the form of different GTPases and protein kinases, several scaffolding proteins that channel incoming signals into different pathways and a variety of phosphatases that modulate MAPK activation dynamics. Thus, depending on the expression and activity states of these proteins, MAPK connections change between cell types and in response to pathological aberrations. In order to analyse the kinetic behaviour and regulation of MAPK cascades we constructed a model which represents a core network of MAPK interactions based on the available literature. The topology of this model is depicted in Fig. 1.

Generally, MAPK systems are arranged in three tiered cascades consisting of MAPKs (lowest tier), MAPK kinases (MAP2Ks, second tier) and MAPK kinases kinases (MAP3Ks, top tier). Activation of the kinases in each tier is modelled with double phosphorylation cycles as described in *Material and Methods* (Sec. 5), in which the upstream kinase acts as the enzyme catalysing the phosphorylation and therefore activation of the downstream kinase. Complementing the classical cascades, the model features several crosstalks and feedbacks (Table 1). First, JNK phosphorylates and activates its own MAP3K (Furuhata et al., 2009; Schachter et al., 2006), generating a positive feedback loop. Second, p38 inhibits ERK activity by enhancing MEK dephosphorylation either via transcriptional upregulation or phosphorylation of protein phosphatase 2 (PP2A) (Junttila et al., 2008; Grethe and Pörn-Ares, 2006; Liu and Hofmann, 2004; Li et al., 2003; Westermarck et al., 2001). Third, ERK inhibits JNK via induction of dual specificity phosphatases (DUSPs) catalysing the dephosphorylation of JNK (Monick et al., 2006; Paumelle et al., 2000). Finally, AKT inhibits JNK

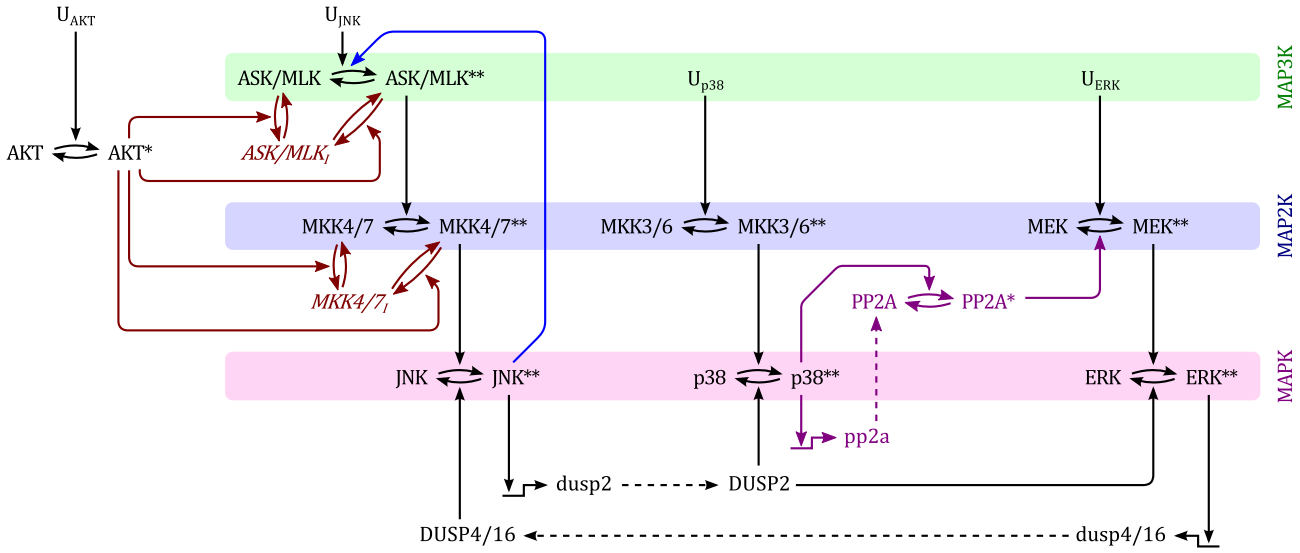

Figure 1: Scheme of the nominal MAPK interaction model. For simplicity of illustration, the double phosphorylation of MAP(K) kinases are depicted in single steps and the three inactive forms of ASK/MLK and MKK4/7 are lumped into one component. U_i denote inputs that are modelled as time-dependent functions (not modelled with differential equations). Black: nominal cascades; Blue: positive feedback from JNK to its own MAP3Ks; Red: negative crosstalk from AKT to JNK signalling; Purple: negative crosstalk from p38 to ERK signalling only occuring in non-transformed cells. Lower- and upper-case letter indicate mRNAs and proteins, respectively. Single and double asterix indicate single- and double-phosphorylated active forms, respectively.

activity by phosphorylating inhibitory sites in the JNK-MAP3Ks and -MAP2Ks (Barthwal et al., 2003; Park et al., 2002; Kim et al., 2001).

In the following section we review experimental evidence for each crosstalk mechanism and show how they are implemented in the dynamic model. Finally, we explore the intricate kinetic behaviour and dynamics of three MAPK cascades.

Stimulus	apparent Hill coefficient		
	HeLa	HEK293	Jurkat
Sorbitol	9	8	4
Anisomycin	10	4	3

Table 2: Ultrasensitivity of the JNK response to stress in mammalian cell populations (Bagowski et al., 2003).

2.1.1 JNK positive feedback

Several studies support the idea of a JNK positive feedback loop on the systems level. For example, JNK positive feedback was critical for a proper stress response of Xenopus oocytes (Bagowski and Ferrell, 2001). In mammalian cells, JNK exhibited all-or-none responses on the single cell level after treatment with anisomycin or sorbitol (Bagowski et al., 2003), and a positive feedback loop was suggested (Bagowski et al., 2003; Xiong and Ferrell, 2003). On the population level, these all-or-none responses manifest highly ultrasensitive behaviour with apparent Hill coefficients as high as 9 or 10 (Table 2), which is consistent with the presence of a positive feedback loop, which increases the degree of ultrasensitivity (Bagowski et al., 2003).

The literature contains considerable evidence supporting the existence of positive feedback from JNK to its own MAP3Ks, in particular to mixed linage kinases (MLK) and apoptosis regulated kinases (ASK) (Furuhata et al., 2009; Schachter et al., 2006; Ventura et al., 2004; Phelan et al., 2001; Xu and Cobb, 1997). For example, in HEK 293, Hela and MCF-7 cells, JNK phosphorylated MLK3 directly at sites in the COOH-terminal region, which resulted in the redistribution of MLK3 to triton-insoluble membrane microdomains, increased phosphorylation of the activation loop and increased MLK3 activity (Schachter et al., 2006). Similarly in COS7 cells, JNK phosphorylated the C-terminal domain of MLK2, which was required for MLK2-induced apoptosis (Phelan et al., 2001). Further, JNK phosphorylated a MEKK1 fragment in vitro and coimmunoprecipitated with MEKK1 in HEK 293 cells Xu and Cobb (1997). MEKK1 is a MAP3K for the JNK pathway, which depending on its phosphorylation status, also can act as a scaffold for the MEKK1-MKK4-JNK pathway (Gallagher et al., 2002).

Another, more indirect route of JNK feeding back to its own MAP3Ks involves the production of reactive oxygen species (ROS). In fibroblasts, JNK produced ROS after TNF treatment, in a process that did not involve gene transcription and was inhibited by NF-κB (Ventura et al., 2004). Interestingly, several signalling pathways connect ROS to JNK activation, suggesting a JNK-ROS positive feedback loop (Shen and Liu, 2006). ASK1 in particular is readily activated by ROS, whereby ROS induces the disso-

Interaction			Mechanism	Comments	References
JNK	→	ASK1	oligomerization and auto-phosphorylation	via JNK induced ROS production (WEHI-231)	Furuhata et al. (2009)
	→	MLK3	phosphorylation	direct JNK mediated phosphorylation (HEK 293, Hela, MCF-7)	Schachter et al. (2006)
p38	⊣	ERK	upregulation of PP2A	only in non-immortalised, non-transformed cells	Junttila et al. (2008); Grethe and Pörn-Ares (2006); Li et al. (2003); Westermarck et al. (2001); Liu and Hofmann (2004)
ERK	⊣	JNK	induction of DUSP4 & DUSP16	MDCK epithelial cells, human alveolar macrophages	Paumelle et al. (2000); Monick et al. (2006)
AKT	⊣	ASK1	phosphorylation at S83	HEK293, L929	Kim et al. (2001)
	⊣	MLK3	phosphorylation at S674	HepG2	Barthwal et al. (2003)
	⊣	MKK4	phosphorylation at S78	HEK293T	Park et al. (2002)
JNK	⊣	ERK, p38	induction of DUSPs via Jun gene transcription, DUSP2 is the speculative isoform assumed in the model.	what DUSP isoforms are involved is unclear; DUSP1,4,6 were not detected in COS7	Peng et al. (2009); Junttila et al. (2008); Stepniak et al. (2006); Shen et al. (2003); Black et al. (2002); Chu et al. (1996)

Table 1: Crosstalks and feedbacks in the nominal MAPK interaction model. The list comprises core-interactions which are supposedly conserved between cell lines, but with the p38-ERK crosstalk being restricted to non-transformed cells. The comments column indicates the experimental system (cell lines) used to identify the links.

ciation of ASK from internal inhibitors such as thioredoxin or 14-3-3 proteins, finally resulting in ASK1 oligomerisation and phosphorylation of its activation loop (Shen and Liu, 2006; Goldman et al., 2004; Saitoh et al., 1998). In fact, such a ROS dependent positive feedback loop has been reported in WEHI-231 mouse B lymphoma cells, where JNK activity produced hydrogen peroxide (H2O2) which, in turn, activated ASK1 (Furuhata et al., 2009).

The molecular mechanisms of MAP3K activation are quite complex. For example, MLK3 activation involves GTPases binding, translocation to the membrane, dimer- or oligomerisation and activation loop phosphorylation of MLK3 at Thr2277 and Ser281 (Schachter et al., 2006). Neglecting this complexity, and in concordance with earlier models in the literature, we model the activation of MAP3Ks as a phosphorylation process catalysed by its inputs (Kholodenko et al., 2010; Kholodenko, 2000). In the model, different JNK-MAP3Ks are lumped into one ASK/MLK component. The activation of this component is modelled as a double phosphorylation cycle with two inputs, representing the activity of upstream GTPases u_3 and active JNK (see Fig. 1). Although our model simplifies the involved molecular events, it captures the main feature of MAP3K activation, namely the phosphorylation of two conserved residues in the activation loop.

2.1.2 p38 inhibits ERK signalling in non-transformed cells

Generally, ERK activity promotes survival. The suppression of this activity by p38 is critical for induction of apoptosis in nontransformed cells and PP2A mediates this effect (Junttila et al., 2008). In particular, p38 mediated dephosphorylation of MEK was necessary for arsenite induced apoptosis in human skin fibroblasts (HSF) and rat primary neurons (CGN), but not in transformed and tumourigenic cell lines (HeLa, Jurkat, K562, HT-1080, WM266-4, A2058) (Li et al., 2003). Further, PP2A mediated this p38-MEK negative crosstalk and was required for both cytokine and stress induced apoptosis in human endothelium cells and rat cardiac ventricular myocytes, respectively (Grethe and Pörn-Ares, 2006; Liu and Hofmann, 2004).

How p38 regulates PP2A is uncertain. PP2A is a heterotrimer composed of a scaffold, a catalytic subunit and different regulatory subunits. Its catalytic activity can be regulated on several levels, including assembly of the heterotrimer with different regulatory subunits, and both phosphorylation or methylation of the catalytic subunit (Nguyen et al., 2012; Janssens and Goris, 2001). Because the mechanism by which p38 upregulates PP2A activity is uncertain, and because the system dynamics depend on this mechanism, our model implements two possibilities, each on opposite ends of the dynamic spectrum: slow upregulation via gene transcription of the regulatory subunit, and fast activation via phosphorylation of the catalytic subunit.

2.1.3 ERK inhibits JNK

ERK signalling strongly induces several DUSPs, some of which negatively regulate JNK activity. For example, DUSP4 is readily induced in response to several growth factors (Cagnol and Rivard, 2012; Legewie et al., 2008) and stabilisation of DUSP16 by ERK mediated phosphorylation at Ser-446 was observed in both COS-7 (fibrob-

lastic) and Hela cells (Katagiri et al., 2005). Further, ERK enhanced JNK dephosphorylation by induction of DUSP4 in Madin-Darby canine kidney (MDCK) epithelial cells (Paumelle et al., 2000) and ERK inhibition in human alveolar macrophages (which are part of the immune system in lung) reduced DUSP16 levels, resulting in increased JNK phosphorylation (Monick et al., 2006). Together, these data indicate that the DUSP4/16 mediated ERK-JNK crosstalk is conserved between cell lines (epithelial, fibroblast, immune and cancer cells) based on which the dynamic model features ERK induced mRNA and protein expression of DUSP4/16 that catalyse the dephosphorylation of JNK.

2.1.4 AKT inhibits JNK signalling

In response to several growth factors and insulin AKT mediates survival signalling, in part, by phosphorylation and inhibition of apoptotic proteins (Hers et al., 2011). Active AKT phosphorylates inhibitory sites of JNK upstream kinases at both the MAP2K and MAP3K level (see Table 1). On the MAP3K level, phosphorylation of ASK1 at Ser 83 by AKT reduced JNK activity in response to oxidative stress and serum starvation, and decreased ASK1 dependent apoptosis in HEK 293 and L929 cells (Kim et al., 2001). Similar results were obtained in HepG2 cells, where insulin induced AKT activity led to phosphorylation of MLK3 at Ser 674 (Barthwal et al., 2003). On the MAP2K level, AKT phosphorylated MKK4 at Ser 78 in response to insulin or constitutively active AKT, which reduced JNK activity and anisomycin induced apoptosis in HEK 293T cells (Park et al., 2002).

The dynamic model does not distinguish different MAP3Ks and MAP2Ks in the JNK pathway, but features combined ASK/MLK and MKK4/7 components, as MAP3Ks and MAP2Ks respectively. We model both components taking a domain oriented approach (Conzelmann et al., 2008; Kiyatkin et al., 2006; Borisov et al., 2006, 2005) and assuming that the phosphorylation processes at the activation loop and the inhibitory site are independent, as described in detail in *Material and Methods*.

2.1.5 JNK inhibits ERK and p38

JNK can inhibit ERK on several levels, involving both indirect upstream mechanisms and direct dephosphorylation upon the transcriptional induction of DUSP expression (Junttila et al., 2008). The model of direct ERK dephosphorylation via transcriptional DUSP induction is supported by two studies showing that the JNK-ERK crosstalk is at least partially independent of the ERK upstream kinases MEK and Raf. First, v-Jun transcriptional activity reduced both basal and growth factor induced ERK phosphorylation at least partially independent of Raf (Black et al., 2002). Second, JNK activity induced by ceramide and TNF-α blocked growth factor stimulated ERK phosphorylation, and this inhibition required c-Jun transcriptional activity but did not involve MEK (Shen et al., 2003).

Although the exact mechanism is poorly understood, and elevated expression of DUSP1, DUSP4 and DUSP6 could not be detected in COS-7 cells expressing active MLK3, DUSPs were suggested as potential mediators of the JNK-ERK crosstalk (Junttila et al., 2008; Shen et al., 2003). JNK can also inhibit p38, as JNK activity inhibited both ERK and p38 signalling in mouse cardiomyocytes (Peng et al., 2009) and c-Jun deficient hepatocytes showed increased phosphorylation of p38 (Stepniak et al., 2006). The JNK $\dashv$ ERK/p38 crosstalk may involve a p53-DUSP2 dependent pathway, as the c-Jun mediated inhibition of p38 observed in hepatocytes was p53 dependent (Stepniak et al., 2006) and DUSP2 was identified as a transcriptional target of p53 in mouse embryonic fibroblast and breast cancer cell lines (Yin et al., 2003). Further, DUSP2 was shown to dephosphorylate ERK and p38 in NIH3T3 and HeLa cells (Chu et al., 1996) and was implicated in the inactivation of ERK2 during p53-dependent apoptosis in breast and colon cancer cell lines (Yin et al., 2003; Dickinson and Keyse, 2006). Based on these data and neglecting p53 as possible intermediate, the dynamic model features JNK induced expression of DUSP2 mRNA and protein and DUSP2-catalysed dephosphorylation of ERK and p38.

2.2 Dynamics of the core network

Based on the model structure in Fig.1 a dynamic model of MAPK interactions can be derived (Kholodenko et al., 2010; Kholodenko, 2006). For detailed introductions to dynamic modelling of cellular systems we refer to Iglesias and Ingalls (2009); Aldridge et al. (2006) and, in particular with regards to ERK/MAPK signalling, Orton et al. (2005); Kolch et al. (2005); Kholodenko (2000). A successful modelling strategy keeps the model simple, yet biologically relevant and capable of meaningful predictions. To that end, the developed model contains several biologically reasonable assumptions, simplifications and generalisations as explained in *Material and Methods* (Sec 5). In particular, the model lumps isoforms and kinases that share the same upstream activators and downstream substrates into a single component wherever possible (Fig. 1). Crucially, the adopted simplifications preserve the network's feedback and crosstalk structures, reduce the risk of over-parameterisation and facilitate the mathematical analysis of the model.

2.2.1 MAPK dynamics in response to growth factors or stress

The developed model reflects the current understanding of how the p38 and JNK systems respond to stress (Junttila et al., 2008), and is consistent with earlier MAPK models in the literature, which, albeit not concerned with p38 and JNK, featured growth factor induced ERK signalling (Kholodenko et al., 2010; Nakakuki et al., 2010; von Kriegsheim et al., 2009). Fig. 2 presents an overview of the system dynamics, illustrating how our model responds to growth factor and stress signals. Generally speaking, growth factors predominantly activate ERK and

JNK, and also AKT, albeit to different extents. The activation dynamics may be sustained or transient, depending on type and context of the stimulation (Nakakuki et al., 2010; von Kriegsheim et al., 2009). For example, PC12 cells exhibit sustained ERK activation in response to NGF, whereas EGF causes transient ERK dynamics due to the activation of several negative feedback loops (von Kriegsheim et al., 2009; Douville and Downward, 1997; Marshall, 1995). These negative feedbacks act upstream of the ERK cascade, at the level of growth factor receptors and their adaptors, and result in a transient input signal for the MAPK system. We can model these transient effects taking a modular approach in which the inputs are modelled by time dependent functions (Nakakuki et al., 2010). Hereby, a step input corresponds to a sustained signal, whereas a pulse input, which drops back to the low basal level after a certain, relatively short time period, corresponds to a transient signal. Fig. 2 panels A and B show that in response to growth factors, the ERK dynamics qualitatively follow the input signal, whereas JNK responds transiently, and only to growth factors that do not activate AKT. Stress signals predominantly activate p38 and JNK and sometimes ERK, but to a much weaker extent. Figure 2C shows that the JNK response to stress is sustained for both transient and sustained stress inputs.

2.2.2 Dynamics of stress induced apoptosis in the presence of growth factors

The core model reflects the current understanding of JNK dependent apoptosis induction. In Junttila et al. (2008) a conceptual model was proposed, in which PP2A mediated suppression of ERK by p38 is critical for JNK mediated apoptosis. The idea is that stress induced activation of p38 suppresses the normal ERK activity of proliferating and differentiating cells and, subsequently, this loss of ERK activity sensitises the cells to JNK mediated apoptosis. Our dynamic model is a mathematical representation of this idea amenable to theoretical analysis. Indeed, simulating the dynamic model with a step input of stress signals

$$u_{\mathrm{p38}}(t) = u_{\mathrm{JNK}}(t) = \begin{cases} 1 & \text{for } t > 0 \\ 0 & \text{otherwise} \end{cases}$$

in the presence of a constant mitotic signal $u_{\mathrm{ERK}}(t) = 1$ mimics the data and sequence of events described in Junttila et al. (2008). Hereby, the qualitative behaviour is largely independent of the exact mechanism of PP2A activation. For both mechanisms, either transcriptional upregulation of PP2A or its activation by p38-induced phosphorylation, the JNK switch occurs at a 3-6 h delay following the apoptotic stimulus (Fig. 3). The delay is largely determined by the strength of the p38-PP2A crosstalk. Decreasing the expression rate of PP2A in the transcriptional upregulation model or decreasing the catalytic activity of p38 towards PP2A in the model of phosphorylation induced PP2A activation increases the time of JNK activation (Fig. 3, dashed lines). In the following, we dissect the MAPK interaction network generating these com-

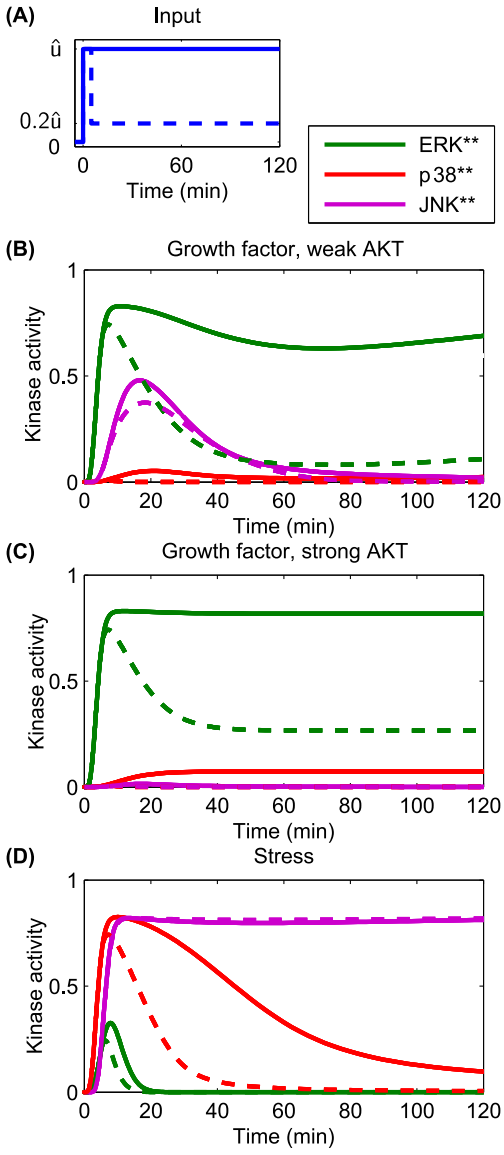

Figure 2: Dynamics of the core network in response to different stimuli. (A) Form of input signals. Solid: sustained input, dashed: transient input. (B-D) System responses for different stimuli. (B) Growth factor strongly stimulating the ERK and JNK inputs, but only weakly the AKT and p38 inputs: (C) Growth factor strongly stimulating the ERK and JNK and AKT inputs, but not the p38 input. (D) Stress signal strongly stimulating the p38 and JNK inputs, weakly stimulating the ERK input and not stimulating the AKT input.

	$\hat{u}_{\mathrm{ERK}}$	$\hat{u}_{\mathrm{p38}}$	$\hat{u}_{\mathrm{JNK}}$	$\hat{u}_{\mathrm{AKT}}$
(B)	1.00	0.15	1.00	0.20
(C)	1.00	0.15	1.00	0.50
(D)	0.50	1.00	1.00	0.00

where $\hat{u}_i$ (i = ERK, p38, JNK) denotes the maximal value of the ERK, p38 and JNK input (see panel A).

plex dynamics, by providing a systems level analysis of these interactions.

2.3 Analysing feedback structures

MAPK systems exhibit complex dynamic behaviour, depending on the topology of feedbacks and kinetic parameters. Although the parameters are important for the responses observed, the network topology in terms of feedback loops determines what qualitative behaviours are possible (Kholodenko, 2006). Generally speaking, negative feedback can generate (sustained) oscillations, whereas positive feedback can generate bistability. Bistability is thought to be important in cell fate decisions, as it is characterised by hysteresis and can generate irreversible switches (Xiong and Ferrell, 2003; Novak and Tyson, 1993). An example is the caspase system, where positive feedback generates an irreversible switch between two stable steady states; an off-state corresponding to survival and an on-state corresponding to apoptosis (Eissing et al., 2004). As the model features a JNK positive feedback loop, we sought to determine under which conditions the system exhibits bistability.

2.3.1 Positive feedback and bistability of the JNK module

A convenient tool for analysing bistability is the loop breaking approach (Angeli et al., 2004). Loop breaking is a graphical analysis tool consisting of two steps. First, break the feedback loop and plot the input/output (i/o) relationship in steady state for the open loop system. The resulting curve is called the steady state characteristic of the open loop. Second, close the loop graphically by plotting a straight line through the origin, whereby the slope of the line represents the inverse strength of the feedback. For example, unitary feedback $u = y$ is represented by a straight line of slope one. The intersection points of the two lines represent the steady states of the closed loop system. In order to assess the stability of the steady states (similarly to nullclines in classical phase plane analysis), two technical prerequisites have to be satisfied; existence of a well-defined i/o characteristic and monotonicity, both of which can be satisfied for simplified MAPK cascades (not exhibiting negative feedback). For details we refer to the original literature (Angeli et al., 2004).

Zooming into the JNK module of the nominal model, the loop breaking approach reveals that the JNK system is indeed bistable for a wide range of feedback strengths (Fig. 4). Note that this result does not depend on the exact parameters, but rather the sigmoidal input-output characteristic of the JNK cascade. In this analysis, the feedback strength corresponds to the catalytic activity of JNK to phosphorylate ASK/MLK. More precisely, let x_0, x_1 and x_2 denote the concentrations of non-, single- and double-phosphorylated ASK/MLK, accordingly, and let further, k_f be the catalytic activity of the upstream ASK/MLK input u and k_b the catalytic activity of active JNK y, then

$$v_{\mathrm{phos,\,i}} = \frac{(k_\mathrm{f}\hat{u} + k_\mathrm{b}\hat{y})x_i}{K_d + x_0 + x_1}, \quad i = 0, 1 \tag{1}$$

describes the rate of ASK/MLK phosphorylation. Hereby, a feedback strength of 100% corresponds to $k_b = k_f$, i.e. equal catalytic activities of input and JNK. Figure 4 shows that for typical values of MAPK phosphorylation and dephosphorylation parameters (Kholodenko et al., 2010; Nakakuki et al., 2010; Kholodenko, 2000; Huang and Ferrell, 1996) the strength of the positive feedback can be reduced to less than 40% before bistability is lost.

The point of transition from monostable to bistable behaviour is called pitchfork bifurcation and depends not only on the feedback strength, but also the upstream input. Recall that ASK/MLK are not only phosphorylated by JNK feedback, but also upstream inputs (such as GTPase recruited kinases or MAP4Ks). For the graphical analysis, assuming a constant input corresponds to a right-shift of the feedback line, whereby the value of the right-shift indicates the strength of the input (Fig. 4). Applying a feedforward input to a feedback system that was originally not bistable (due to a low feedback gain), can push it into a bistable regime and beyond. Hereby the system moves from a monostable-off regime through a bistable regime to a monostable-on regime (Fig. 4). Further, a combined analysis of feedback and feedforward input shows that even for appropriate inputs, bistability is lost if the feedback strength is too low. In fact, in order for a bistable regime to exist, the inverse of the feedback strength has to be smaller than the maximal slope of the sigmoidal i/o characteristic (Fig. 4).

2.3.2 Negative feedback via dual specificity kinases

The core model depicted in Fig 1 does not contain negative feedback within the JNK module. However, negative feedback is not uncommon in MAPK cascades and is often context dependent. For instance, ERK possesses several negative feedback loops that are activated in a stimulation dependent manner in response to EGF, but not NGF or HRG (Nakakuki et al., 2010; von Kriegsheim et al., 2009; Santos et al., 2007). With regard to JNK signalling, several DUSPs exhibit catalytic activity towards JNK and may be induced by active JNK (Boutros et al., 2008; Dickinson and Keyse, 2006). One such example is DUSP1 (Bokemeyer et al., 1996). Therefore, we explored the possibility of DUSP1 mediated negative feedback in the JNK module. Note that the system is not monotonic because of the negative feedback. Consequently, graphical analysis using loop breaking cannot assess the stability of the steady states but only their existence and should be complemented by local stability analysis or simulations.

Negative feedback to upstream components of JNK can decrease ultrasensitivity and lead to oscillations (data not shown, see for example Kholodenko et al. (2010) for a general treatment). In contrast, DUSP1 mediated, slow negative feedback can disable the bistable switch generated by

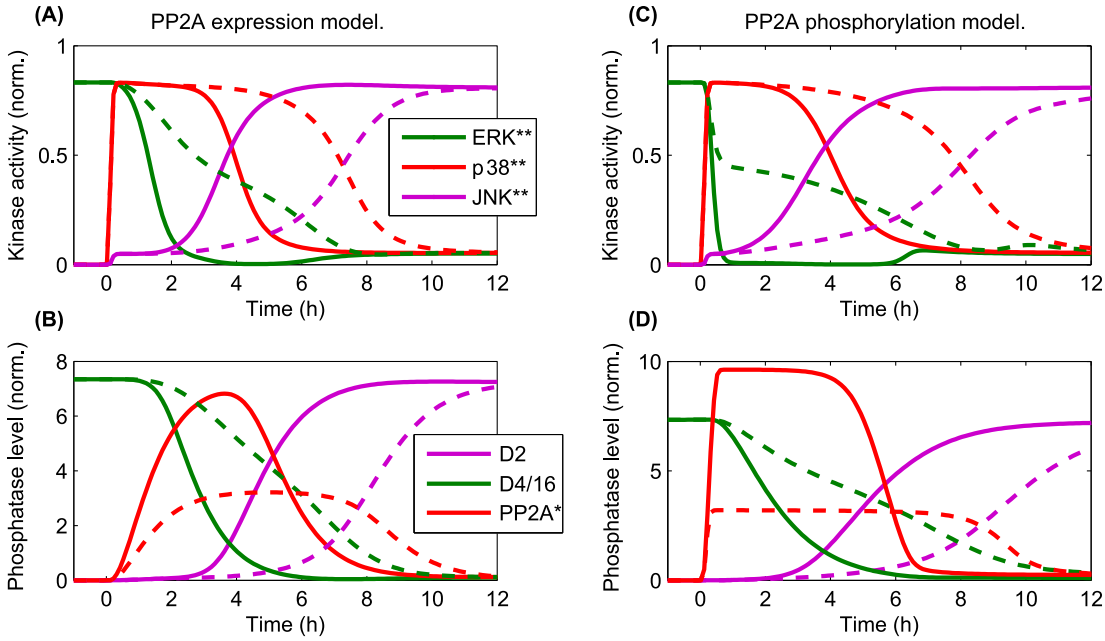

Figure 3: Trajectories of the core model mimic the sequence of events Junttila et al. (2008) that occur in response to a stress stimulus $u_{\mathrm{p38}}(t) = u_{\mathrm{JNK}}(t) = 1$ for $t > 0$ and the presence of a constant mitotic signal $u_{\mathrm{ERK}}(t) = 1$ for all t. D2 and D4/16 denote DUSP2 and DUSP4/16, which mediate the JNK ⊣ ERK, p38 and ERK ⊣ JNK crosstalks, respectively (see also Table 1). The qualitative behaviour is independent of the mechanistic details implementing p38-PP2A interaction. Two mechanism are shown: (A,B) p38 induces PP2A gene expression, whereby the red line in panel B represents the total level of PP2A protein, (C,D) p38 phosphorylates PP2A, whereby the red line in panel D represents phosphorylated PP2A. (A-D) The timing of JNK activation depends on the strength of PP2A upregulation: Solid lines indicate PP2A levels comparable to those of the other phosphatases. Dashed lines indicate reduced levels of PP2A expression, which delays JNK activation.

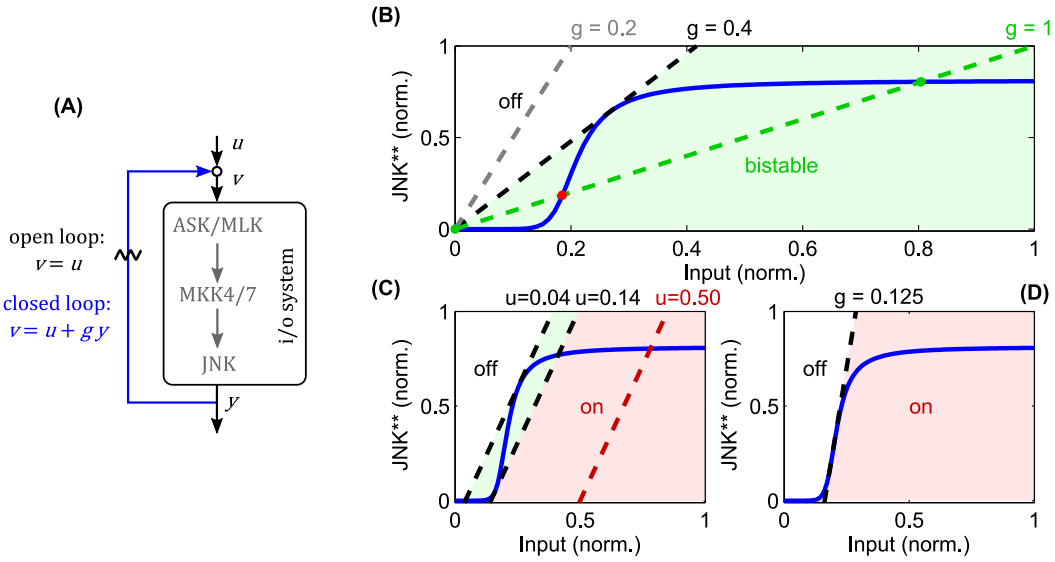

Figure 4: Analysis of JNK positive feedback using the loop breaking approach. Here, g denotes the feedback strength, i.e. the ratio $g = k_{\mathrm{b}}/k_{\mathrm{f}}$ in (1). (A-D) Solid, blue lines represent the steady-state characteristic of i/o-system. Dashed lines indicate different feedback configurations, whereby the slope represents the feedback strength and the right-shift measured from the origin the feedforward stimulus. (A) Illustration of the loop breaking approach (for a detailed explanation see main text) (B) Depending on the feedback strength, the JNK system exhibits monostable or bistable behaviour (u=0). (C) Simultaneous feedback and feedforward stimulation can push the system from a monostable-off (white), through a bistable (light green), to a monostable-on (light red) regime. (D) No bistable behaviour is possible for feedback gains lower than the inverse of the maximal slope of the i/o characteristic.

the fast positive feedback loop (Fig.5). Depending on the relative feedback strength, a transiently bistable regime exists, in which the JNK system responds with prolonged activity in response to a short lived stimulus. Hereby, the positive feedback maintains the on-state after the input subsides, but only until the slow negative feedback takes effect, diminishing the (initial) i/o characteristic of the system, at which point JNK switches off (Fig.5).

2.4 Regulation of the JNK apoptotic switch by crosstalk

Mitogenic and survival signals regulate the JNK apoptotic switch through crosstalk occurring on several levels (Fig. 1). We can distinguish two mechanisms; firstly, inhibition of JNK activation by phosphorylation of upstream JNK kinases at inhibitory residues and secondly enhanced JNK dephosphorylation by upregulation of phosphatases. The first mechanism is mediated by AKT, a classical mediator of survival signalling. The second mechanism, is mediated via ERK, a classical mediator of proliferative and differentiation signalling.

In the following, we use the nominal model to decipher how MAPK crosstalk integrates different mitotic, survival and stress signals, particularly focusing on the bistable switch. First, we stimulate the model with constant mitotic and survival inputs $u_{\mathrm{ERK}}(t) = \hat{u}_{\mathrm{ERK}}, u_{\mathrm{AKT}}(t) = \hat{u}_{\mathrm{AKT}}$ and let the trajectories relax to steady state. Then we apply stress stimuli in the form of step inputs

$$u_{\mathrm{p38}}(t) = \begin{cases} 0 & \text{for } t < 0 \\ \hat{u}_{\mathrm{p38}} & \text{otherwise,} \end{cases}$$

$$u_{\mathrm{JNK}}(t) = \begin{cases} 0 & \text{for } t < 0 \\ \hat{u}_{\mathrm{JNK}} & \text{otherwise.} \end{cases}$$

It is useful to define the switching threshold as the value of $\hat{u}_{\mathrm{JNK}}$ at which JNK switches from the off to the on state.

2.4.1 How AKT controls the JNK switch

AKT signalling affects the switching threshold and regulates the JNK on-state (Fig. 6). Increasing AKT activity decreases the value of the JNK on-state. Whereas bistable behaviour is still possible for moderate AKT signalling, strong AKT signalling abrogates the JNK apoptotic switch and permits only moderate, proliferative JNK activity.

The regulation of the JNK switch by AKT does not depend on the exact topology of the crosstalk, as isolated crosstalk at the MAP2K or the MAP3K levels exhibits similar control patterns (Fig. 6). One slight difference is that crosstalk on the MAP3K level has slightly more impact on the switching threshold and admits some sensitivity of the proliferative regime with respect to the JNK input, meaning that changing the JNK input changes the level of JNK activity (orange and red curves in Fig. 6B). In contrast, the curves resulting from the MAP2K crosstalk are almost flat, meaning that changing the JNK input does not affect JNK activity other than switching it on or off (Fig. 6C). Thus, the MAP2K crosstalk model quickly saturates for all levels of AKT activity, after which changing the input has no effect on the output. In contrast, the MAP3K crosstalk model does not saturate when AKT activity is high, and after crossing a certain threshold, JNK responds linearly to changes in the input.

2.4.2 How ERK and p38 control the JNK switch

Increasing the input of ERK signalling shifts the switching-threshold towards higher JNK inputs, but has little effect on the value of the on-state (Fig. 7). Crucially, no intermediate JNK activation is possible, JNK is either off or on, Further, the strength of apoptotic JNK signalling once activated, is independent of the ERK input.

The regulation of the JNK switch by ERK depends on the p38-ERK crosstalk, p38 $\rightarrow$ PP2A $\dashv$ ERK. Normal, nontransformed cells can initiate the JNK apoptotic switch depending on the level of PP2A expression and p38 signalling. Here, increasing p38 pathway activation and PP2A expression increases the regime of tolerable ERK stimuli for which JNK inputs can initiate the apoptotic switch (Fig. 7B). In contrast, in transformed and tumourigenic cells, lacking p38-ERK crosstalk, even very moderate stimulation of the ERK pathway prevents the JNK apoptotic switch (Fig. 7C).

2.4.3 How different DUSP-mediated crosstalk patterns shape JNK dynamics

DUSPs are important regulators of MAPK activities. The main function of DUSPs is to dephosphorylate the activation loop of MAPKs, often with overlapping substrate specificity (Bermudez et al., 2010; Boutros et al., 2008; Dickinson and Keyse, 2006). Importantly, several DUSPs are in turn regulated by MAPKs and induced in response to mitotic, differentiation and stress signals. Therefore, the regulation of DUSPs can occur on several levels including the regulation of DUSP phosphatase activity, substrate specificity, protein stability and gene expression (Boutros et al., 2008; Dickinson and Keyse, 2006). The resulting feedback and crosstalk structures are complex, and lack a complete understanding. Owing to this complexity, we formulated several models based on reported DUSP specificities in the literature (Tab. 3, Patterson et al. (2009); Boutros et al. (2008); Dickinson and Keyse (2006)). By focusing on MAPK induced gene transcription and neglecting the complexity of posttranscriptional DUSP regulations, these models are used to analyse the effects of different crosstalk structures.

DUSP1 expression can be induced by active p38 and JNK depending on the cell context (Tab. 3), and it is often upregulated in cancer. The JNK-induced DUSP1 expression and the resulting negative feedback onto JNK was already analysed in Sec. 2.3.2, Fig.5. In this section we focus on the p38 induced DUSP1 expression and resulting p38 $\dashv$ p38/JNK crosstalk. We have already seen in Sec. 2.4.2, Fig. 7 that p38 $\dashv$ ERK $\dashv$ JNK crosstalk is a critical regulator of the JNK switch. However, the core model also features JNK $\dashv$ ERK/p38 crosstalk mediated

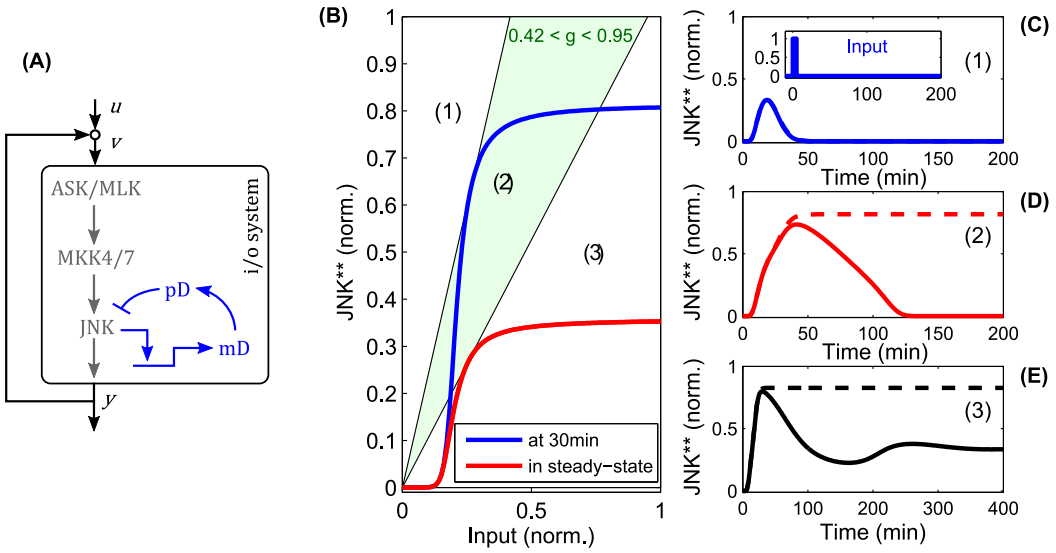

Figure 5: Modulation of the bistable switch by negative feedback. (A) Scheme of the extended JNK model, in which active JNK induces the expression of DUSP1 mRNA (mD) and protein (pD). (B) Loop breaking analysis showing a transient bistable regime (light green). Blue: initial i/o characteristic of the open loop system at $t = 30$min, before the negative feedback takes effect. Red: steady-state i/o characteristic. (C-E) Trajectories of the JNK response after stimulation with a transient pulse of 3min ($u(t) = 1$ for $0 < t < 3$) for different feedback strengths: (C) $g = 0$, (D) $g = 0.7$, (E) $g = 1.5$. Dashed lines indicate the responses without negative feedback, solid lines with negative feedback.

by DUSP2 expression, and we ask whether this crosstalk is also crucial for the JNK switch by deleting DUSP2 in the model.

Figure 8 shows the responses for different crosstalk patterns to step inputs of stress signals,

$$u_{\mathrm{p38}}(t) = u_{\mathrm{JNK}}(t) = \begin{cases} 1 & \text{for } t > 0 \\ 0 & \text{otherwise} \end{cases}$$

in the presence of a constant mitotic signal $u_{\mathrm{ERK}}(t) = 1$ for all t. We can distinguish two qualitatively different behaviours, irrespective of the presence or absence of ERK feedback (mediated by DUSP4 or DUSP5/6). The models in the first group do not feature p38 induced DUSP1 expression, and DUSP2 deletion in these models has little effect on the JNK activation dynamics and the JNK switch (Fig. 8A,B). Within this group, model A is the core model, but model B also includes DUSP4 mediated negative feedback to ERK; ERK ⊣ ERK/JNK (Tab. 3), resulting in accelerated JNK activation dynamics (Fig. 8B). In contrast, the models in the second group feature p38 induced DUSP1 expression, and deletion of DUSP2 in these models abrogates the JNK switch, resulting in reduced, moderate JNK activity (Fig. 8C-E). In addition to the core interactions, model C includes this p38 induced DUSP1 expression, which slightly delays the JNK activation dynamics, but does not obliterate the JNK switch (Fig. 8C). However, deleting DUSP2 in model C abrogates the JNK switch and results in only moderate JNK activity (Fig. 8C). Summarising, these models predict that abrogation of JNK dependent apoptosis requires both p38 induced expression of DUSP1 and downregulation or deletion of DUSP2. Adding ERK negative feedback mediated by DUSP4 (model D) or DUSP4 and DUSP5/6 (model E) to model C does not alter the JNK dynamics or the behaviour of the DUSP2 deletion (Fig. 8D,E).

The robustness of the core model with respect to either i) gain of p38 induced DUSP1 or ii) loss of JNK induced DUSP2 in isolation, can be explained as follows. To lock JNK into the highly active state (in the presence of ERK input), ERK activity needs to be supressed, either by p38 activity via the PP2A-ERK link or by JNK activity via the DUSP2-ERK link. In the absence of DUSP1, p38 activity is sufficiently high to supress ERK. In presence of DUSP1, the p38 activity is reduced and ERK is not sufficiently supressed by p38-PP2A alone. Here, the JNK-DUSP2-ERK crosstalk becomes crucial as it complements the p38-PP2A mediated ERK inhibition, which explains the fragility of the JNK switch if both elevation of p38-induced DUSP1 and loss of JNK-induced DUSP2 occur simultaneously

3 Discussion

The process of building a multi-pathway model is quite complex, as are the implications of its analysis for cell biology and cancer. Both are discussed in the following.

3.1 Theoretical considerations

The network depicted in Fig 1 synthesises information from different cell types in the literature. However, a complete picture of MAPK crosstalk is still lacking. The network of DUSP interactions is particularly difficult to dis-

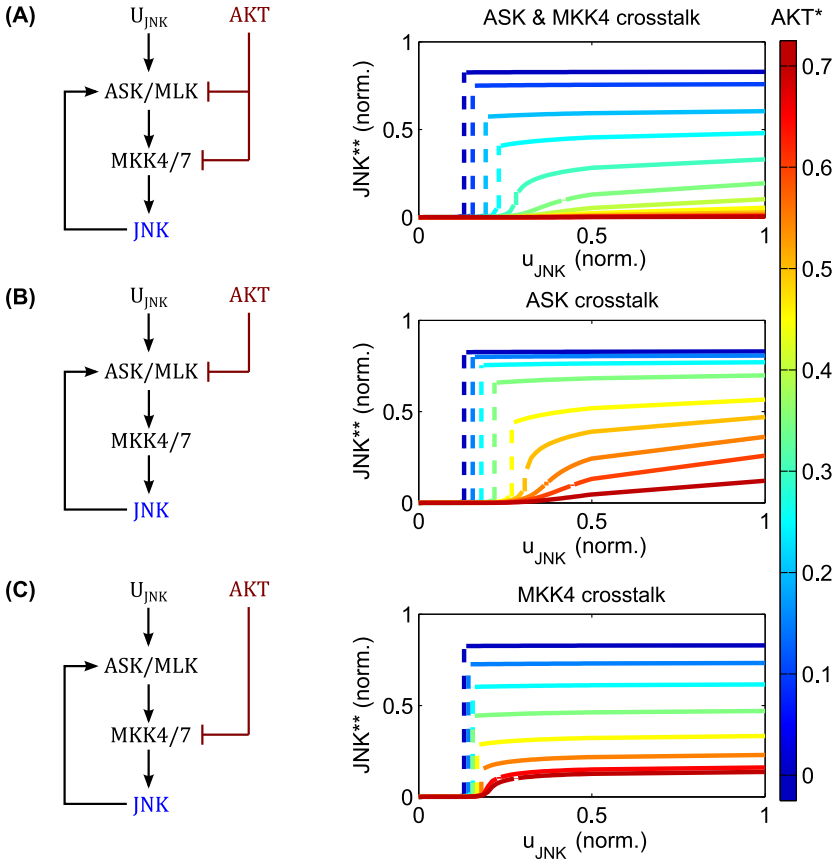

Figure 6: Regulation of switch by AKT negative crosstalk. (A-C) Interaction schemes and simulated dose responses for crosstalk at different levels: MAP3K and MAP2K level (A); MAP3K level (B) and MAP2K level (C), whereby active AKT phosphorylates and inhibits ASK/MLK and/or MKK4/7 as indicated. Left: Interaction scheme. Right: Dose responses with respect to the JNK input u_{JNK} for different AKT activation levels; $u_{\mathrm{JNK}}(t) = \hat{u}_{\mathrm{JNK}}$ for $t > 0$; $u_{\mathrm{AKT}} = \hat{u}_{\mathrm{AKT}}$ for all t; blue curves indicate low, red lines high AKT activity; dashed lines indicate a switch from low to high JNK activity.

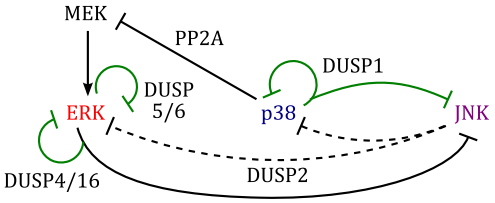

	Model configuration		
	DUSP5/6	DUSP1	DUSP4/16
(A)	-	-	ERK ⊣ JNK
(B)	-	-	ERK ⊣ JNK,ERK
(C)	-	p38 ⊣ JNK,p38	ERK ⊣ JNK
(D)	-	p38 ⊣ JNK,p38	ERK ⊣ JNK,ERK
(E)	ERK ⊣ ERK	p38 ⊣ JNK,p38	ERK ⊣ JNK,ERK

All models DUSP2: JNK ⊣ ERK, p38 & PP2A: p38 ⊣ MEK

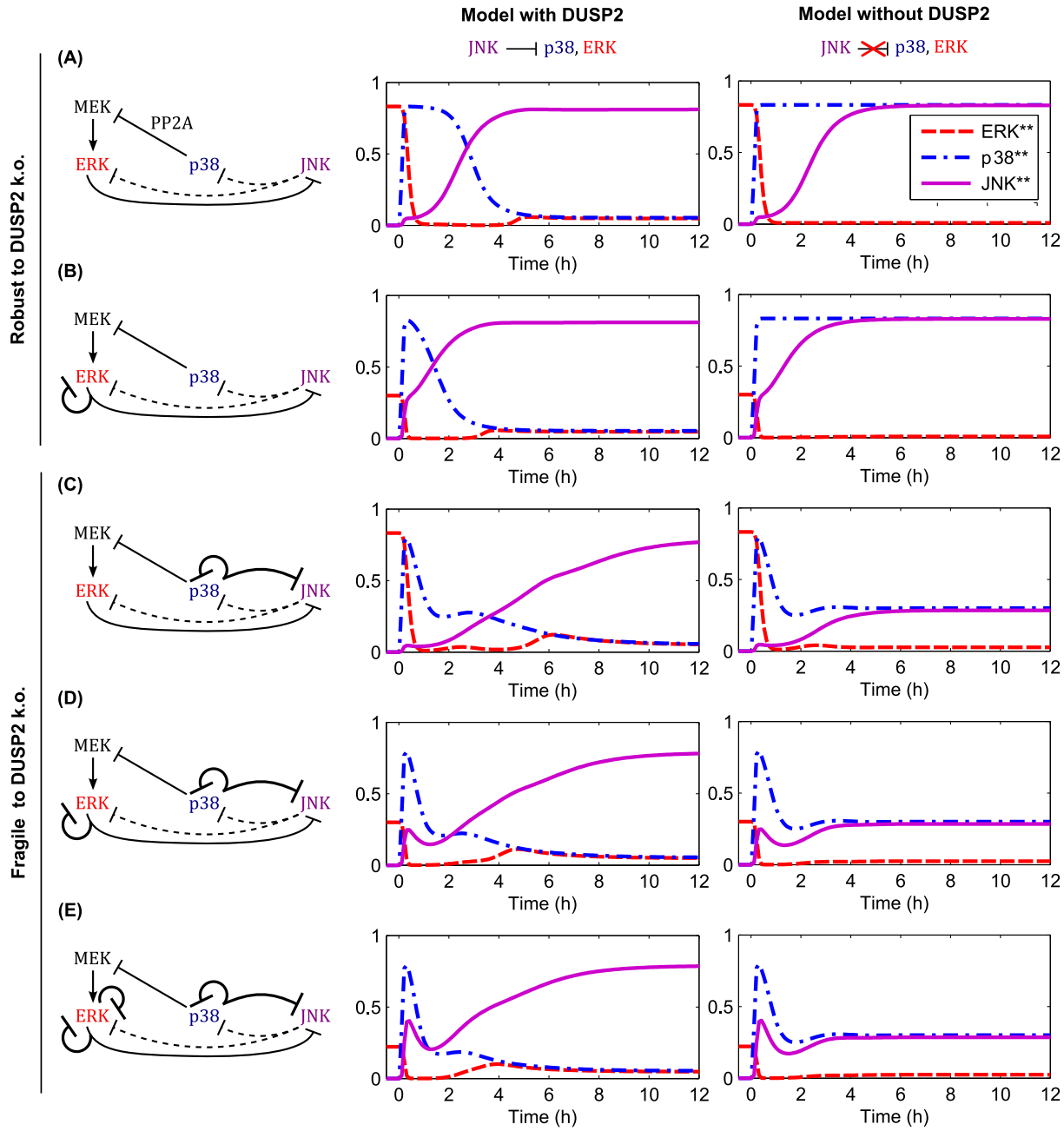

Figure 8: Dynamics of the apoptotic switch for different crosstalk patterns. Centre and right columns show the trajectories of MAPKs activation after a stress stimulus ($u_{\mathrm{p38}} = u_{\mathrm{JNK}} = 1\,\mathrm{for}\,t > 0$) in the presence of a mitotic signal ($u_{\mathrm{ERK}} = 1\,\mathrm{for\ all}\,t$) for the indicated interaction patterns. Top left: Scheme of MAPK interactions. Black arcs indicate core interactions, green arcs indicate additional DUSP mediated interactions analysed in panels (A-E). Top right: Table summarising the different DUSP interaction patterns corresponding to panels (A-E). (A) Core model (see Fig. 1 for a detailed scheme) (B) Core model and DUSP4 mediated negative feedback on ERK. (C) Core model and p38 induced DUSP1 expression mediating negative feedback to ERK and crosstalk to JNK: p38 ⊣ p38/JNK. (D) Model C and DUSP4 mediated negative feedback on ERK. (E) Model D and DUSP5/6 mediated negative feedback on ERK.

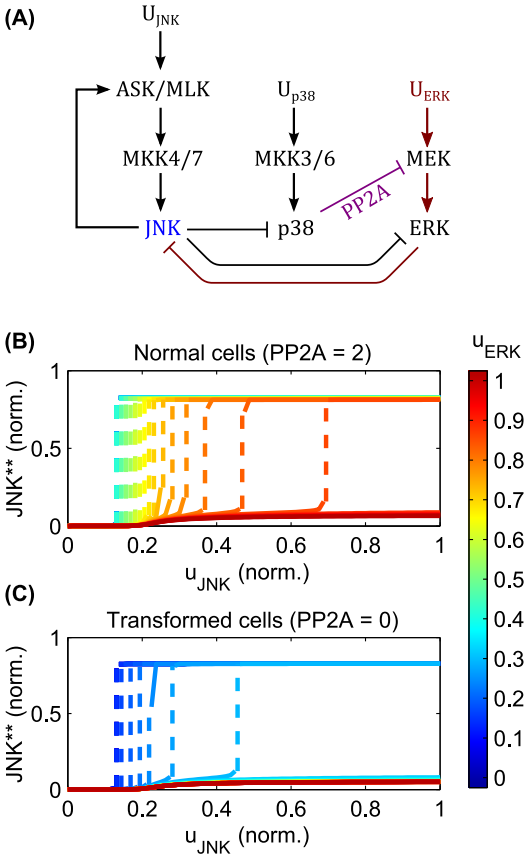

Figure 7: Regulation of th JNK switch by ERK and p38. (A) Interaction scheme. (B-C) Simulated dose responses with respect to the JNK inputs for different levels of constant ERK pathway stimulation; $u_{\mathrm{JNK}}(t) = \hat{u}_{\mathrm{JNK}}$ for $t > 0$; $u_{\mathrm{p38}}(t) = 1$ for $t > 0$; $u_{\mathrm{ERK}} = \hat{u}_{\mathrm{ERK}}$ for all t; blue curves indicate low, red lines high ERK stimulation; dashed lines indicate a switch from low to high JNK activity. (B) Dose responses for primary/nontransformed cells exhibiting p38 ⊣ ERK crosstalk. (C) Dose responses for transformed/tumourigenic cells lacking the p38 ⊣ ERK crosstalk (no PP2A upregulation in the model).

sect, as DUSPs can be induced by several MAPKs and, in turn, can act on several substrates (Boutros et al., 2008). Importantly, Fig 1 is not an overview summarising all possible interactions, but depicts a core model of MAPK interactions that are essential for implementing the JNK proliferative-apoptotic switch. From a systems-theoretical perspective, the crucial determinant of the model's behaviour is that these crosstalks and feedbacks exists, not which molecules mediate it. Therefore, although all interactions in the model are strongly supported by experimental evidence in the literature, the particular DUSP isoforms involved may differ depending on cell type and context. The DUSP2 connection in our model is based on data from fibroblast and cancer cell lines (see Sec. 2.1.5), but is particularly uncertain. DUSP2 specifically dephosphorylated ERK and p38 in NIH3T3 and HeLa cells (Chu et al., 1996), but targeted JNK in macrophages and mast cells (Jeffrey et al., 2006). These differences suggest that the JNK ⊣ ERK/p38 crosstalk may be mediated differently in immune cells compared to fibroblasts and epithelial cancer cells. In concordance with our model, macrophages and mast cells exhibited JNK ⊣ ERK/p38 crosstalk, but unlike our model this crosstalk was not mediated by DUSP2, as DUSP2 deletion in macrophages and mast cells increased JNK activity and decreased ERK and p38 phosphorylation (Jeffrey et al., 2006). These cell type specific differences highlight the importance of flexible modelling approaches that facilitate the analysis of different model configurations. As illustrated in Section 2.4.3, testing alternative model topologies can readily be done by setting parameters in the current model.

3.1.1 Modularity and neglected components

The nominal model neglects several context dependent MAPK crosstalks and feedbacks that are not necessary for implementing the JNK apoptotic switch. For example, ERK features several (negative) feedback loops (von Kriegsheim et al., 2009; Birtwistle et al., 2007). Generally, this feedback acts upstream of MEK (on the components that are not included in the model, such as growth factor receptors, their adaptors and GTPases), thereby transiently shaping Raf activation, i.e. the input of the model u_1. Thus, although the model does not account for ERK feedbacks explicitly, it can account for different Raf activation patterns by choosing u_1 accordingly as a time-dependent input function (Nakakuki et al., 2010). One advantage of this modular approach is that it facilitates further model development as the input functions can be replaced by additional sets of differential equations. Therewith, the model can be easily connected to other models describing the dynamics of different receptors and GTPases.

Future model development will concern including more mechanistic detail, in particular with regard to the well-studied ERK cascade. For instance, ERK exhibits a strong negative feedback to Raf-1 in response to EGF which alters the efficiency of MEK inhibition (Sturm et al., 2010) and might affect the p38-PP2A-MEK crosstalk. In con-

DUSP	induced by	substrates	comments/references
DUSP4/16	**ERK** (JNK)	**JNK**, ERK	Oncogenic Ras activity induces DUSP4 mRNA and protein synthesis and stabilises DUSP4 protein (Cagnol and Rivard, 2012); ERK phosphorylation stabilises DUSP16 protein, which dephosphorylate JNK>>p38>ERK, mRNA expression was not analysed (Katagiri et al., 2005)
DUSP2	**JNK** (ERK)	**ERK**, **p38**	JNK/c-Jun activity and transformed v-JUN enhances ERK dephosphorylation (Shen et al., 2003; Black et al., 2002); DUSP2 was implicated in regulating the JNK ⊣ ERK/p38 crosstalk (Jeffrey et al., 2006); DUSP2 dephosphorylates ERK and p38 (Dickinson and Keyse, 2006)
DUSP1	p38 (ERK, JNK)	p38, JNK	p38 induces DUSP1, which dephosphorylates p38 and JNK (Hu et al., 2007; Small et al., 2007); DUSP1 mRNA is induced by p38 in response to heat shock (marcophages) (Wong et al., 2005), anisomycin (VSMC) (Bokemeyer et al., 1998), arsenite, UVC (C3H 10T1/2) (Li et al., 2001); and by ERK in response to serum (CCL-39) (Brondello et al., 1997), PDGF, phorbol ester, angiotensin II (VSMC) (Bokemeyer et al., 1998), heat shock, H2O2 (C3H 10T1/2) (Li et al., 2001); and by JNK after stress (NIH 3T3) (Bokemeyer et al., 1996)
DUSP5/6	ERK	ERK	MEK/ERK but not PI3K/AKT or p38/JNK regulates DUSP6 mRNA (stabilisation) and protein (destabilisation) levels (Bermudez et al., 2011) Ras and ERK activity induces dusp5 mRNA and regulates DUSP5 protein stability (Cagnol and Rivard, 2012; Kucharska et al., 2009)

Table 3: Inducible DUSPs implemented in the model. Bold face indicate activities used in the nominal model. Normal face indicate activities used in Sec. 2.4.3. Round brackets indicate activities not used in this study but implemented in the model, wherewith the model is readily adaptable to cell type and cancer specific interaction patterns by setting the parameters in the model accordingly (see also Tab. 5).

trast, IGF predominantly activates ERK via B-Raf without featuring negative feedback (Fritsche-Guenther et al., 2011), illustrating that these model extensions will be context and stimulus dependent.

3.1.2 Spatial aspects

Mathematically, the model describes the cell as well mixed compartment and does not distinguish subcellular compartments. This simplification might not be an issue for the ERK-JNK crosstalk as it features both a nuclear (DUSP4) and a cytosolic (DUSP16) component, but might overestimate the effects of the JNK-ERK/p38 and p38-JNK crosstalks, because their mediators DUSP2 and DUSP1 are exclusively localised in the nucleus. In general, the spatial regulation of DUSPs and MAPKs is complex, as DUSPs can both shuttle and sequester MAPKs in the nucleus and cytosol (Caunt and Keyse, 2012; Mandl et al., 2005; Karlsson et al., 2004; Masuda et al., 2001). In addition, many MAPKs and their MAP2Ks also shuttle between the cytosol and nucleus, and activation and deactivation can take place in both compartments (Plotnikov et al., 2011). For instance, MKK3/6 are located both in the cytosol and nucleus and can mediate p38 activation in the nucleus (Ben-Levy et al., 1998). Both ERK and MEK constitutively shuttle between the cytosol and nucleus, and ERK can be activated in both compartments (Fujioka et al., 2006). Likewise, ERK deactivation by DUSPs can occur in the nucleus and cytosol depending on the localisation of particular DUSP isoforms. Nuclear DUSPs seem to serve as anchoring proteins that retain dephosphorylated ERK in the nucleus to prevent re-activation in the cytosol (Lenormand et al., 1998). Thus, spatial context seems to play an intricate role in modulation of MAPK activities, more work would will be needed to decipher and model the spatial regulations of DUSPs and their effects on MAPK activities.

3.1.3 Parameter dependency

The parameterisation of dynamic models is complex, usually requiring time-course measurements in several different conditions and fitting of the model using global optimisation algorithms, whereby the resulting parameter estimates might vary depending on cell type and experimental context. To obtain a nominal model, we chose the parameters values in concordance with earlier models of MAPK signalling and kinetic information in the literature, such as half-life measurements of DUSPs (see *Material and Methods*). For simplification, the model assumed equal parameters for different MAPKs. We do not expect this assumption to withstand experimental validation during parameter estimation as it was adopted for theoretical reasons. (We refer to Cirit et al. (2010); von Kriegsheim et al. (2009); Nakakuki et al. (2010) for compilations of kinetic parameters and Legewie et al. (2008) for turnover rates.) First, assuming equal binding constants for kinases acting on shared substrates established symmetries in the model that yielded simplified, Michaelis-Menten-like kinetic expressions in a model reduction step (see *Material and Methods*). Second, choosing equal catalytic activities for the different MAPKs simplifies analysing the model based on the rationale that, in this case, the system dynamics are dominated by the systems structure and not biased towards possible imbalances of particular parameter values. Nonetheless, an important feature of the model is that the bistable nature of the JNK apoptotic switch does not depend on the exact parameter values used, but relies on feedback structure and sigmoidal shape of the i/o-characteristic. Nevertheless, in order to achieve a quantitatively predictive model, future work would be needed for data collection and parameterisation, particularly with regard to stress activated kinases where little kinetic information is available.

3.2 Biological implications

Although the idea of a JNK positive feedback loop is not new (Ventura et al., 2006), a detailed understanding of how JNK feedback structures and crosstalk regulate cell fate is still missing (Wagner and Nebreda, 2009). Earlier modelling studies considered MAPK systems in isolation from each other, either focusing on ERK signalling and its feedbacks (Kholodenko et al., 2010; Sturm et al., 2010; Nakakuki et al., 2010; von Kriegsheim et al., 2009), or p38-JNK crosstalk (Sundaramurthy and Gakkhar, 2010; Sundaramurthy et al., 2009). In contrast, this manuscript provides a systems level model of JNK positive feedback, its regulation by pathway crosstalk including ERK and AKT signalling, and a mathematical analysis of how this system integrates different proliferative, survival and proapoptotic stimuli, thereby determining cell fates. The model helps us to understand the experimental observations in the literature, and incorporates several ideas. First, the magnitude and temporal profile of JNK signalling is important, as the anti-apoptotic, proliferative response is associated with moderate, but rapid JNK activation, whereas the proapoptotic response is associated with later, more sustained JNK activation (Ventura et al., 2006; Lamb et al., 2003; Sakon et al., 2003). Second, both mitotic signalling via ERK and survival signalling via AKT modulate the JNK apoptotic switch (Junttila et al., 2008; Molton et al., 2003). Third, the loss of negative crosstalk from p38 to ERK dysregulates JNK dependent apoptosis, which is crucial for cell transformation (Junttila et al., 2008; Arroyo and Hahn, 2005). Overall, JNK signalling involving a positive feedback loop takes a centre stage in the proposed model, which explains how ERK and AKT mediated crosstalk modulates and switches proliferative and proapoptotic JNK signalling

3.2.1 Differences of ERK and AKT control over the JNK apoptotic switch

In the model, the switch to apoptotic JNK signalling depends crucially on a JNK positive feedback loop, which, once activated, causes high levels of sustained JNK activity. This switch is modulated by ERK and AKT signalling in different ways. ERK activity shifts the threshold for the JNK apoptotic switch to higher values, but has no

effect on the strength of apoptotic JNK signalling. The mechanism underlying this behaviour is the enhanced dephosphorylation of JNK, whereby JNK activity is either sufficient to activate the JNK positive feedback loop and inhibit ERK signalling, or does not reach this threshold level. In contrast, AKT activity predominantly regulates the strength of JNK signalling by reducing the value of the JNK-on-state with little effect on the switching threshold. The mechanism behind this is the phosphorylation and inhibition of JNK upstream kinases, which reduces the strength of both, the feedforward loop and the feedback loop. Crucially, the reduced feedback strength yields a reduced level of the JNK-on state.

3.2.2 Transformed versus normal cells

Transformed cell differ from normal cells in that they lack PP2A mediated negative crosstalk from p38 to ERK (Junttila et al., 2008). In the model, the loss of p38-ERK negative crosstalk severely increases the JNK switching threshold, thus desensitising the cells from stress induced apoptosis. Taken together, these observations suggest the involvement of the JNK apoptotic switch in cellular senescence as follows. With each cell cycle, cells accumulate DNA damage and experience a shortening of the chromosomal telomeres. Once a certain threshold of DNA damage or telomere shortening is crossed, senescence occurs or apoptosis is induced. The loss of p38-ERK crosstalk would increase this threshold to unphysiological levels, thus rendering transformed cells biologically immortal. In this senescence model, AKT is not involved, as the AKT-JNK crosstalk does not alter the apoptotic threshold, but, instead, prevents the apoptotic switch in the presence of survival signals.

4 Conclusions

The developed model explains how pathway crosstalk harmonises MAPK responses resulting in pivotal cell fate decisions that differ markedly between transformed and non-transformed cells. In the proposed model, JNK can switch from a transient to sustained activity due to multiple positive feedback loops. Once activated, positive feedback locks JNK into a highly active state that promotes cell death. The switch is differentially regulated by the ERK, p38 and AKT pathways. ERK activation enhances the dual specify phosphatase (DUSP) mediated dephosphorylation of JNK and shifts the threshold of the apoptotic switch to higher inputs. In nontransformed cells, activation of p38 can restore the threshold by inhibiting ERK activity via the phosphatases PP1 or PP2A. Finally, AKT activation inhibits the JNK positive feedback, thus abrogating the apoptotic switch and allowing only proliferative signalling. The model is most valuable for understanding how cancerous deregulations disturb the signal-processing of internal and external cues and provides possible explanations for certain drug resistances. For instance, oncogene induced ERK hyperactivity prevents the normal apoptotic switch and provides possible explanations for the complex and tumour specific behaviour of MAPK systems (Bermudez et al., 2010; Wagner and Nebreda, 2009; Dickinson and Keyse, 2006).

In regards to interactions necessary for facilitating the switch between transient and sustained JNK activity, our model predicts a critical role for DUSP1 and DUSP2 expression patterns. In the model, both expression of DUSP1 and deletion of DUSP2 are necessary for preventing the JNK apoptotic switch (as the nominal model is robust to dysregulation of either DUSP in isolation). The result is particularly interesting in the context of a) cancer, as many cancers show increased expression of DUSP1 and reduced expression of DUSP2, and b) tumour related conditions such as hypoxia, where low oxygen levels upregulate DUSP1 and downregulate DUSP2 (Lin et al., 2011; Patterson et al., 2009). According to our model, these conditions would prevent the JNK apoptotic switch. Indeed, forced expression of DUSP2 abolished hypoxia induced chemoresistance in human cancer cell lines (Lin et al., 2011), and inhibition of DUSP1 sensitised several resistant cancer cell lines to JNK dependent apoptosis (Wang et al., 2008; Small et al., 2007; Snchez-Prez et al., 2000; Laderoute et al., 1999).

The current model represents a core network of MAPK interactions critical for the switch from proliferative to apoptotic signalling. The model is canonical in the sense that it generalises and integrates information from different cell lines by focusing on interactions that are a) readily observed in several cell lines and b) important for controlling the JNK bistable switch. The canonical model forms a basis for experimental design and can be tailored to different experimental systems on two levels by a) parameter estimation (the epigenetic and disease background of particular cell types is reflected in different parameter values of the model) and b) extending the model to incorporate different MAPK isoforms, upstream and downstream signalling and scaffolds. Such refined and validated models possess quantitative predictive power and cannot only be used for identifying gaps in knowledge by testing the model predictions, but also for predicting the effect of drugs, thus building the theoretical basis for identifying optimal treatment strategies.

5 Material and Methods

This section describes how the different components depicted in Fig. 1 are modelled mathematically.

5.1 Model of kinase activation

Activation of mitogen activated protein kinases requires the phosphorylation of two conserved amino acid residues, whereby several upstream kinases can act as enzymes facilitating the phosphorylation. Consider the reaction scheme in Fig. 9, where we assumed that only one enzyme can be bound to the kinase at any one time. Using the law of

mass action the reaction rates are described by

$$r_1 = p_1 x_0 u_1 - p_{-1} x_{0u1}, \tag{2a}$$
$$v_1 = k_1 x_{0u1}, \tag{2b}$$
$$r_2 = p_1 x_1 u_1 - p_{-1} x_{1u1}, \tag{2c}$$
$$v_2 = k_1 x_{1u1}, \tag{2d}$$
$$r_3 = p_2 x_0 u_2 - p_{-2} x_{0u2}, \tag{2e}$$
$$v_3 = k_2 x_{0u2}, \tag{2f}$$
$$r_4 = p_2 x_1 u_1 - p_{-2} x_{1u2}, \tag{2g}$$
$$v_4 = k_2 x_{1u2}, \tag{2h}$$

and the dynamics of the system are governed by the ordinary differential equations

$$\frac{dx_0}{dt} = -r_1 - r_3, \tag{3a}$$
$$\frac{dx_1}{dt} = v_1 - r_2 + v_3 - r_4, \tag{3b}$$
$$\frac{dx_2}{dt} = v_2 + v_4, \tag{3c}$$
$$\frac{dx_{0u1}}{dt} = r_1 - v_1, \tag{3d}$$
$$\frac{dx_{1u1}}{dt} = r_2 - v_2, \tag{3e}$$
$$\frac{dx_{0u2}}{dt} = r_3 - v_3, \tag{3f}$$
$$\frac{dx_{1u2}}{dt} = r_4 - v_4. \tag{3g}$$

We can obtain a simplified description of this system resembling classical Michaelis Menten kinetics using the conserved moieties for the enzymes

$$u_i = \hat{u}_i - x_{0ui} - x_{1ui}, \quad (i = 1, 2),$$

where $\hat{u}_i$ denotes the total concentration of enzyme i, and assuming rapid equilibrium for the binding reactions by solving the system $r_i = 0$ $(i = 1, \ldots, 4)$ for the complexed states $x_{0u1}, x_{1u1}, x_{0u2}, x_{1u2}$. Substituting the solution into the phosphorylation reactions v_i $(i = 1, \ldots, 4)$ yields

$$v_1 = \frac{\hat{u}_1 k_1 x_0}{K_{d1} + x_0 + x_1}, \tag{4a}$$
$$v_2 = \frac{\hat{u}_1 k_1 x_1}{K_{d1} + x_0 + x_1}, \tag{4b}$$
$$v_3 = \frac{\hat{u}_2 k_2 x_0}{K_{d2} + x_0 + x_1}, \tag{4c}$$
$$v_4 = \frac{\hat{u}_2 k_2 x_1}{K_{d2} + x_0 + x_1}, \tag{4d}$$
$$\tag{4e}$$

with $K_{di} = p_{-i}/p_i$ $(i = 1, 2)$ denoting the dissociation constant of the enzyme-kinase complexes. We can further simplify the model by assuming equal dissociation constants $K_{di} = K_d$, wherewith

$$v_{\text{phos1}} = v_1 + v_3 = \frac{(k_1 \hat{u}_1 + k_2 \hat{u}_2) x_0}{K_d + x_0 + x_1},$$
$$v_{\text{phos2}} = v_2 + v_4 = \frac{(k_1 \hat{u}_1 + k_2 \hat{u}_2) x_1}{K_d + x_0 + x_1}.$$

Assuming equal dissociation constants is a strong assumption, in particular for different enzymes, but reduces the risk of over-parameterisation and facilitates the theoretical analysis of the model.

Dephosphorylation of kinases is catalysed by phosphatases and a mathematical model can be derived analogously, resulting in kinetic expressions resembling (5). Therewith, a complete model of a double phosphorylation cycle is given by

$$\frac{d}{dt}x_0 = -\sum_i (k_i \hat{u}_i) \frac{x_0}{K_d + x_0 + x_1} + \sum_j (k_{-j} \hat{v}_j) \frac{x_1}{K_{-d} + x_1 + x_2},$$
$$\frac{d}{dt}x_2 = \sum_i (k_i \hat{u}_i) \frac{x_1}{K_d + x_0 + x_1} - \sum_j (k_{-j} \hat{v}_j) \frac{x_2}{K_{-d} + x_1 + x_2},$$

where u_i denote the concentrations of the upstream kinases, v_j the concentrations of the phosphatases.

5.2 Model of kinase inhibition by phosphorylation

Some kinases can be rendered catalytically inactive by phosphorylation at inhibitory sites. Examples are ASK1 and MKK4, which can be phosphorylated by AKT at Ser 83 and Ser 78, respectively (Kim et al., 2001; Park et al., 2002). There is little, mostly conflicting information available on whether phosphorylation of the inhibitory site depends on the phosphorylation status of the activating sites, or, in turn, whether phosphorylation at the inhibitory site affects the phosphorylation/dephosphorylation of the activating sites. Hence, we take a domain oriented approach accounting for all possible combinations of the phosphorylation status (but neglecting the possibility of a trimeric complex), resulting in a model comprising six distinct states (Conzelmann et al., 2008; Kiyatkin et al., 2006; Borisov et al., 2006, 2005).

Assume that the phosphorylation status of the activating site does not affect the binding of the inhibitor enzyme and the phosphorylation of the inhibitory site, and vice versa that the phosphorylation status of the inhibitory site does not affect the binding of of the activating enzyme and the phosphorylation of the activating site. Assume further, that only one enzyme can be bound to the kinase at any one time, i.e. a trimeric complex consisting of activating enzyme, kinase and inhibitory enzyme is not possible. Then the reaction scheme in Fig. 9 can be extended to account for kinase inhibition:

$$X_i \underset{}{\overset{U_I}{\rightleftharpoons}} X_{iI}, \quad (i = 0, 1, 2),$$

where X_{iI} denotes the kinase phosphorylated at the inhibitory site and U_i the enzyme catalysing this phosphorylation.

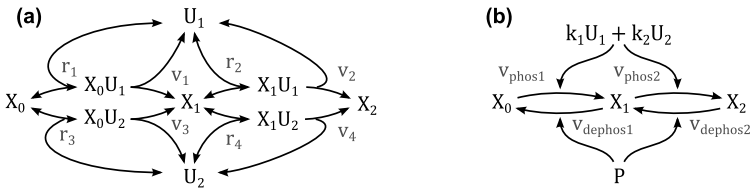

Figure 9: Schemes of a double phosphorylation cycle with two kinases. X denotes the protein to be phosphorylated with the index indicating its phosphorylation status. U denote the kinases catalysing the phosphorylations. (A) Full mechanistic scheme modelled using mass action kinetics. For clarity of presentation, the dephosphorylation reactions are not depicted. (B) Reduced scheme modelled using Michaleis-Menten type kinetics as derived in the main text; k_1 and k_2 denote the catalytic activity of U_1 and U_2, respectively. P denotes the phosphatase catalysing the dephosphorylation.

Similarly to (5) a mathematical description can be derived, yielding reaction kinetics for (de-)phosphorylation at the activating sites of the form

$$r_{\text{phos}} = \frac{\sum_l k_l \hat{u}_l y}{K_d + x_0 + x_1 + x_{0I} + x_{1I}},$$
$$r_{\text{dephos}} = \frac{\sum_l k_{-l} \hat{v}_{-l} z}{K_{-d} + x_1 + x_2 + x_{1I} + x_{2I}},$$

where $(y, z) \in \{(x_0, x_1), (x_1, x_2), (x_{0I}, x_{1I}), (x_{0I}, x_{1I})\}$ and reaction kinetics for (de-)phosphorylation of the inhibitory site of the form

$$r_{\text{phos,I}} = \frac{k_I \hat{u}_I y}{K_I + x_0 + x_1 + x_2},$$
$$r_{\text{dephos,I}} = \frac{k_{-I} \hat{v}_I z}{K_{-I} + x_{0I} + x_{1I} + x_{2I}},$$

where $(y, z) \in \{(x_0, x_{0I}), (x_1, x_{1I}), (x_2, x_{2I})\}$.

5.3 Model of phosphatase expression

The expression levels of inducible phosphatases depend on several parameters, including the activities of upstream MAPKs (Fig 1). We model the rate of mRNA synthesis using sigmoidal Hill functions of activator kinase concentrations (motivated by thermostatistical arguments (Frank et al., 2012)) and assume first order kinetics for translation and degradation rates. Therewith a dynamic model of gene expression is described as

$$\frac{d}{dt}x = k_{\text{synt}} \frac{u^n}{K^n + u^n} - k_{\text{deg}} x,$$
$$\frac{d}{dt}y = p_{\text{synt}} x - p_{\text{deg}} y,$$

where u denotes the concentration of upstream kinase activity, x and y denote mRNA and protein concentrations, respectively, and k_{synt}, K, n, k_{deg}, p_{synt} and p_{deg} are kinetic parameters. Many of these parameters can be fixed based on biologically reasonable assumptions and kinetic data available in the literature.

The half life of several unmodified DUSP proteins were reported as beeing between 20 and 45 min (DUSP1,4,5,6,16). However, following postranslational regulation by phosphorylation and ubiquitination, these half lives ranged from as short as 7.5 min to as long as 4 h (Cagnol and Rivard, 2012; Kucharska et al., 2009; Katagiri et al., 2005). The half live of DUSP6 mRNA was reported as beeing between 20 to 40 min, which decreased to as little as 8 min following the inhibiton of basal MEK activity (Bermudez et al., 2011). Neglecting this complexity, the model assumes equal half lives for protein and mRNA at a value of 30 min for all phosphatases, which fixes the degradation parameters according to $k_{\text{deg}} = p_{\text{deg}} = log(2)/(30\text{min})$. Further, the model assumes a 10-fold amplification from the mRNA level to the protein level, fixing the protein synthesis parameter according to $p_{\text{synt}} = 10 p_{\text{deg}}$. The expression level of mRNA was normalised ($x \leq 1$), which fixes the mRNA synthesis parameter at $p_{\text{synt}} = k_{\text{deg}}$. The remaining parameters were chosen such that for strong, constant activity of the upstream kinase yields reasonable expression levels of around 80% ($x \approx 0.8$) of the maximal possible value. Further assuming a reasonable degree of ultrasensitivity $n = 2$, fixes the threshold of half activation at $K = 0.5$

6 Acknowledgments

The research leading to these results has received funding from the Science Foundation Ireland under grant No. 06/CE/B1129, and the European Union Seventh Framework Programme (FP7/2007-2013) ASSET project under grant agreement number FP7-HEALTH-2010-259348.

References

Aldridge, B. B., J. M. Burke, D. A. Lauffenburger, and P. K. Sorger (2006, Nov). Physicochemical modelling of cell signalling pathways. *Nat Cell Biol 8*(11), 1195–1203.

Angeli, D., J. E. Ferrell, and E. D. Sontag (2004, Feb). Detection of multistability, bifurcations, and hysteresis in a large class of biological positive-feedback systems. *Proc Natl Acad Sci U S A 101*(7), 1822–1827.

Arroyo, J. D. and W. C. Hahn (2005, Nov). Involvement of PP2A in viral and cellular transformation. *Oncogene 24*(52), 7746–7755.

Reaction	Forward rate law	Reverse rate law	K_d	K_{-d}	k_1	k_{-1}	k_2	k_{-2}	k_{-3}
			unitless		min^{-1}	min^{-1}	min^{-1}	min^{-1}	min^{-1}
$\mathrm{MEK} \underset{\mathrm{PP2A}^*}{\overset{\mathrm{U_{ERK}}}{\rightleftharpoons}} \mathrm{MEK}^*$	$\frac{k_1 \mathrm{U_{ERK}} \mathrm{MEK}}{K_d+\mathrm{MEK}+\mathrm{MEK}^*}$	$\frac{k_{-1} \mathrm{PP2A}^* \mathrm{MEK}^*}{K_{-d}+\mathrm{MEK}^*+\mathrm{MEK}^{**}}$	1	1	1	0.25	-	-	-
$\mathrm{MEK}^* \underset{\mathrm{PP2A}^*}{\overset{\mathrm{U_{ERK}}}{\rightleftharpoons}} \mathrm{MEK}^{**}$	$\frac{k_1 \mathrm{U_{ERK}} \mathrm{MEK}^*}{K_d+\mathrm{MEK}+\mathrm{MEK}^*}$	$\frac{k_{-1} \mathrm{PP2A}^* \mathrm{MEK}^{**}}{K_{-d}+\mathrm{MEK}^*+\mathrm{MEK}^{**}}$	1	1	1	0.25	-	-	-
$\mathrm{ERK} \underset{\mathrm{D2,D4/16,D5/6}}{\overset{\mathrm{MEK}^{**}}{\rightleftharpoons}} \mathrm{ERK}^*$	$\frac{k_1 \mathrm{MEK}^{**} \mathrm{ERK}}{K_d+\mathrm{ERK}+\mathrm{ERK}^*}$	$\frac{(k_{-1}\mathrm{D2}+k_{-2}\mathrm{D4/16}+k_{-3}\mathrm{D5/6})\mathrm{ERK}^*}{K_{-d}+\mathrm{ERK}^*+\mathrm{ERK}^{**}}$	1	1	1	0.25	-	0	0
$\mathrm{ERK}^* \underset{\mathrm{D2,D4/16,D5/6}}{\overset{\mathrm{U_{ERK}}}{\rightleftharpoons}} \mathrm{ERK}^{**}$	$\frac{k_1 \mathrm{U_{ERK}} \mathrm{ERK}^*}{K_d+\mathrm{ERK}+\mathrm{ERK}^*}$	$\frac{(k_{-1}\mathrm{D2}+k_{-2}\mathrm{D4/16}+k_{-3}\mathrm{D5/6})\mathrm{ERK}^{**}}{K_{-d}+\mathrm{ERK}^*+\mathrm{ERK}^{**}}$	1	1	1	0.25	-	0	0
$\mathrm{MKK3/6} \overset{\mathrm{U_{p38}}}{\rightleftharpoons} \mathrm{MKK3/6}^*$	$\frac{k_1 \mathrm{U_{p38}} \mathrm{MKK3/6}}{K_d+\mathrm{MKK3/6}+\mathrm{MKK3/6}^*}$	$\frac{k_{-1} \mathrm{MKK3/6}^*}{K_{-d}+\mathrm{MKK3/6}^*+\mathrm{MKK3/6}^{**}}$	1	1	1	0.25	-	-	-
$\mathrm{MKK3/6}^* \overset{\mathrm{U_{p38}}}{\rightleftharpoons} \mathrm{MKK3/6}^{**}$	$\frac{k_1 \mathrm{U_{p38}} \mathrm{MKK3/6}^*}{K_d+\mathrm{MKK3/6}+\mathrm{MKK3/6}^*}$	$\frac{k_{-1} \mathrm{MKK3/6}^{**}}{K_{-d}+\mathrm{MKK3/6}^*+\mathrm{MKK3/6}^{**}}$	1	1	1	0.25	-	-	-
$\mathrm{p38} \underset{\mathrm{D1,D2}}{\overset{\mathrm{MKK3/6}^{**}}{\rightleftharpoons}} \mathrm{p38}^*$	$\frac{k_1 \mathrm{MKK3/6}^{**} \mathrm{p38}}{K_d+\mathrm{p38}+\mathrm{p38}^*}$	$\frac{(k_{-1}\mathrm{D1}+k_{-2}\mathrm{D2})\mathrm{p38}^*}{K_{-d}+\mathrm{p38}^*+\mathrm{p38}^{**}}$	1	1	1	0	-	0.25	-
$\mathrm{p38}^* \underset{\mathrm{D1,D2}}{\overset{\mathrm{MKK3/6}^{**}}{\rightleftharpoons}} \mathrm{p38}^{**}$	$\frac{k_1 \mathrm{MKK3/6}^{**} \mathrm{p38}^*}{K_d+\mathrm{p38}+\mathrm{p38}^*}$	$\frac{(k_{-1}\mathrm{D1}+k_{-2}\mathrm{D2})\mathrm{p38}^{**}}{K_{-d}+\mathrm{p38}^*+\mathrm{p38}^{**}}$	1	1	1	0	-	0.2	-
$\mathrm{ASK} \overset{\mathrm{U_{JNK}}}{\rightleftharpoons} \mathrm{ASK}^*$	$\frac{(k_1 \mathrm{U_{JNK}}+k_{-2}\mathrm{JNK}^{**})\mathrm{ASK}}{K_d+\mathrm{ASK}+\mathrm{ASK}^*+\mathrm{ASK}_I+\mathrm{ASK}_I^*}$	$\frac{k_{-1} \mathrm{ASK}^*}{K_{-d}+\mathrm{ASK}^*+\mathrm{ASK}^{**}+\mathrm{ASK}_I^*+\mathrm{ASK}_I^{**}}$	1	1	1	0.25	1	-	-
$\mathrm{ASK}^* \overset{\mathrm{U_{JNK}}}{\rightleftharpoons} \mathrm{ASK}^{**}$	$\frac{(k_1 \mathrm{U_{JNK}}+k_{-2}\mathrm{JNK}^{**})\mathrm{ASK}^*}{K_d+\mathrm{ASK}+\mathrm{ASK}^*+\mathrm{ASK}_I+\mathrm{ASK}_I^*}$	$\frac{k_{-1} \mathrm{ASK}^{**}}{K_{-d}+\mathrm{ASK}^*+\mathrm{ASK}^{**}+\mathrm{ASK}_I^*+\mathrm{ASK}_I^{**}}$	1	1	1	0.25	1	-	-
$\mathrm{ASK}_I \overset{\mathrm{U_{JNK}}}{\rightleftharpoons} \mathrm{ASK}_I^*$	$\frac{(k_1 \mathrm{U_{JNK}}+k_{-2}\mathrm{JNK}^{**})\mathrm{ASK}_I}{K_d+\mathrm{ASK}+\mathrm{ASK}^*+\mathrm{ASK}_I+\mathrm{ASK}_I^*}$	$\frac{k_{-1} \mathrm{ASK}_I^*}{K_{-d}+\mathrm{ASK}^*+\mathrm{ASK}^{**}+\mathrm{ASK}_I^*+\mathrm{ASK}_I^{**}}$	1	1	1	0.25	1	-	-
$\mathrm{ASK}_I^* \overset{\mathrm{U_{JNK}}}{\rightleftharpoons} \mathrm{ASK}_I^{**}$	$\frac{(k_1 \mathrm{U_{JNK}}+k_{-2}\mathrm{JNK}^{**})\mathrm{ASK}_I^*}{K_d+\mathrm{ASK}+\mathrm{ASK}^*+\mathrm{ASK}_I+\mathrm{ASK}_I^*}$	$\frac{k_{-1} \mathrm{ASK}_I^{**}}{K_{-d}+\mathrm{ASK}^*+\mathrm{ASK}^{**}+\mathrm{ASK}_I^*+\mathrm{ASK}_I^{**}}$	1	1	1	0.25	1	-	-
$\mathrm{ASK} \overset{\mathrm{AKT}^*}{\rightleftharpoons} \mathrm{ASK}_I$	$\frac{k_1 \mathrm{AKT}^* \mathrm{ASK}}{K_d+\mathrm{ASK}+\mathrm{ASK}^*+\mathrm{ASK}^{**}}$	$\frac{k_{-1} \mathrm{ASK}_I}{K_{-d}+\mathrm{ASK}_I+\mathrm{ASK}_I^*+\mathrm{ASK}_I^{**}}$	1	1	1	0.25	-	-	-
$\mathrm{ASK}^* \overset{\mathrm{AKT}^*}{\rightleftharpoons} \mathrm{ASK}_I^*$	$\frac{k_1 \mathrm{AKT}^* \mathrm{ASK}^*}{K_d+\mathrm{ASK}+\mathrm{ASK}^*+\mathrm{ASK}^{**}}$	$\frac{k_{-1} \mathrm{ASK}_I^*}{K_{-d}+\mathrm{ASK}_I+\mathrm{ASK}_I^*+\mathrm{ASK}_I^{**}}$	1	1	1	0.25	-	-	-
$\mathrm{ASK}^{**} \overset{\mathrm{AKT}^*}{\rightleftharpoons} \mathrm{ASK}_I^{**}$	$\frac{k_1 \mathrm{AKT}^* \mathrm{ASK}^{**}}{K_d+\mathrm{ASK}+\mathrm{ASK}^*+\mathrm{ASK}^{**}}$	$\frac{k_{-1} \mathrm{ASK}_I^{**}}{K_{-d}+\mathrm{ASK}_I+\mathrm{ASK}_I^*+\mathrm{ASK}_I^{**}}$	1	1	1	0.25	-	-	-
$\mathrm{MKK4/6} \overset{\mathrm{ASK}^{**}}{\rightleftharpoons} \mathrm{MKK4/6}^*$	$\frac{k_1 \mathrm{ASK}^{**} \mathrm{MKK4/6}}{K_d+\mathrm{MKK4/6}+\mathrm{MKK4/6}^*+\mathrm{MKK4/6}_I+\mathrm{MKK4/6}_I^*}$	$\frac{k_{-1} \mathrm{MKK4/6}^*}{K_{-d}+\mathrm{MKK4/6}^*+\mathrm{MKK4/6}^{**}+\mathrm{MKK4/6}_I^*+\mathrm{MKK4/6}_I^{**}}$	1	1	1	0.25	-	-	-
$\mathrm{MKK4/6}^* \overset{\mathrm{ASK}^{**}}{\rightleftharpoons} \mathrm{MKK4/6}^{**}$	$\frac{k_1 \mathrm{ASK}^{**} \mathrm{MKK4/6}^*}{K_d+\mathrm{MKK4/6}+\mathrm{MKK4/6}^*+\mathrm{MKK4/6}_I+\mathrm{MKK4/6}_I^*}$	$\frac{k_{-1} \mathrm{MKK4/6}^{**}}{K_{-d}+\mathrm{MKK4/6}^*+\mathrm{MKK4/6}^{**}+\mathrm{MKK4/6}_I^*+\mathrm{MKK4/6}_I^{**}}$	1	1	1	0.25	-	-	-
$\mathrm{MKK4/6}_I \overset{\mathrm{ASK}^{**}}{\rightleftharpoons} \mathrm{MKK4/6}_I^*$	$\frac{k_1 \mathrm{ASK}^{**} \mathrm{MKK4/6}_I}{K_d+\mathrm{MKK4/6}+\mathrm{MKK4/6}^*+\mathrm{MKK4/6}_I+\mathrm{MKK4/6}_I^*}$	$\frac{k_{-1} \mathrm{MKK4/6}_I^*}{K_{-d}+\mathrm{MKK4/6}^*+\mathrm{MKK4/6}^{**}+\mathrm{MKK4/6}_I^*+\mathrm{MKK4/6}_I^{**}}$	1	1	1	0.25	-	-	-
$\mathrm{MKK4/6}_I^* \overset{\mathrm{ASK}^{**}}{\rightleftharpoons} \mathrm{MKK4/6}_I^{**}$	$\frac{k_1 \mathrm{ASK}^{**} \mathrm{MKK4/6}_I^*}{K_d+\mathrm{MKK4/6}+\mathrm{MKK4/6}^*+\mathrm{MKK4/6}_I+\mathrm{MKK4/6}_I^*}$	$\frac{k_{-1} \mathrm{MKK4/6}_I^{**}}{K_{-d}+\mathrm{MKK4/6}^*+\mathrm{MKK4/6}^{**}+\mathrm{MKK4/6}_I^*+\mathrm{MKK4/6}_I^{**}}$	1	1	1	0.25	-	-	-
$\mathrm{MKK4/6} \overset{\mathrm{AKT}^*}{\rightleftharpoons} \mathrm{MKK4/6}_I$	$\frac{k_1 \mathrm{AKT}^* \mathrm{MKK4/6}}{K_d+\mathrm{MKK4/6}+\mathrm{MKK4/6}^*+\mathrm{MKK4/6}^{**}}$	$\frac{k_{-1} \mathrm{MKK4/6}_I}{K_{-d}+\mathrm{MKK4/6}_I+\mathrm{MKK4/6}_I^*+\mathrm{MKK4/6}_I^{**}}$	1	1	1	0.25	-	-	-
$\mathrm{MKK4/6}^* \overset{\mathrm{AKT}^*}{\rightleftharpoons} \mathrm{MKK4/6}_I^*$	$\frac{k_1 \mathrm{AKT}^* \mathrm{MKK4/6}^*}{K_d+\mathrm{MKK4/6}+\mathrm{MKK4/6}^*+\mathrm{MKK4/6}^{**}}$	$\frac{k_{-1} \mathrm{MKK4/6}_I^*}{K_{-d}+\mathrm{MKK4/6}_I+\mathrm{MKK4/6}_I^*+\mathrm{MKK4/6}_I^{**}}$	1	1	1	0.25	-	-	-
$\mathrm{MKK4/6}^{**} \overset{\mathrm{AKT}^*}{\rightleftharpoons} \mathrm{MKK4/6}_I^{**}$	$\frac{k_1 \mathrm{AKT}^* \mathrm{MKK4/6}^{**}}{K_d+\mathrm{MKK4/6}+\mathrm{MKK4/6}^*+\mathrm{MKK4/6}^{**}}$	$\frac{k_{-1} \mathrm{MKK4/6}_I^{**}}{K_{-d}+\mathrm{MKK4/6}_I+\mathrm{MKK4/6}_I^*+\mathrm{MKK4/6}_I^{**}}$	1	1	1	0.25	-	-	-
$\mathrm{JNK} \underset{\mathrm{D1,D4/16}}{\overset{\mathrm{MKK4/6}^{**}}{\rightleftharpoons}} \mathrm{JNK}^*$	$\frac{k_1 \mathrm{MKK4/6}^{**} \mathrm{JNK}}{K_d+\mathrm{JNK}+\mathrm{JNK}^*}$	$\frac{(k_{-1}\mathrm{D1}+k_{-2}\mathrm{D4/16})\mathrm{JNK}^*}{K_{-d}+\mathrm{JNK}^*+\mathrm{JNK}^{**}}$	1	1	1	0	-	0.25	-
$\mathrm{JNK}^* \underset{\mathrm{D1,D4/16}}{\overset{\mathrm{MKK4/6}^{**}}{\rightleftharpoons}} \mathrm{JNK}^{**}$	$\frac{k_1 \mathrm{MKK4/6}^{**} \mathrm{JNK}^*}{K_d+\mathrm{JNK}+\mathrm{JNK}^*}$	$\frac{(k_{-1}\mathrm{D1}+k_{-2}\mathrm{D4/16})\mathrm{JNK}^{**}}{K_{-d}+\mathrm{JNK}^*+\mathrm{JNK}^{**}}$	1	1	1	0	-	0.25	-
$\mathrm{AKT} \overset{\mathrm{U_{AKT}}}{\rightleftharpoons} \mathrm{AKT}^*$	$\frac{k_1 \mathrm{U_{AKT}} \mathrm{AKT}}{K_d+\mathrm{AKT}}$	$\frac{k_{-1} \mathrm{AKT}^*}{K_{-d}+\mathrm{AKT}^*}$	1	1	1	0.25	-	-	-
$\mathrm{PP2A} \overset{\mathrm{p38}^{**}}{\rightleftharpoons} \mathrm{PP2A}^*$	$\frac{k_1 \mathrm{p38}^{**} \mathrm{PP2A}}{K_d+\mathrm{PP2A}}$	$\frac{k_{-1} \mathrm{PP2A}^*}{K_{-d}+\mathrm{PP2A}^*}$	1	1	1	0.25	-	-	-

Table 4: Reactions, rate expressions and parameters of the (de-)phosphorylation processes in the core model. For simplicity ASK in the table denotes ASK/MLK in the model.

Reaction	Forward rate law	Reverse rate law	K unitless	k_{synt} min^{-1}	k_{deg} min^{-1}	α	β	γ
						unitless		
$\varnothing \underset{}{\overset{\text{p38,JNK}}{\rightleftharpoons}}$ dusp1	$k_{\text{synt}} \frac{(\alpha \text{p38}+\beta \text{JNK})^2}{K^2+(\alpha \text{p38}+\beta \text{JNK})^2}$	k_{deg}dusp1	0.5	0.0231	0.0231	1	0	0
$\varnothing \underset{}{\overset{\text{dusp1}}{\rightleftharpoons}}$ DUSP1	k_{synt}dusp1	k_{deg}DUSP1	-	0.231	0.0231	-	-	-
$\varnothing \underset{}{\overset{\text{ERK,JNK}}{\rightleftharpoons}}$ dusp2	$k_{\text{synt}} \frac{(\alpha \text{ERK}+\beta \text{JNK})^2}{K_d^2+(\alpha \text{ERK}+\beta \text{JNK})^2}$	k_{deg}dusp2	0.5	0.0231	0.0231	0	1	0
$\varnothing \underset{}{\overset{\text{dusp2}}{\rightleftharpoons}}$ DUSP2	k_{synt}dusp1	k_{deg}DUSP1	-	0.231	0.0231	-	-	-
$\varnothing \underset{}{\overset{\text{ERK,JNK}}{\rightleftharpoons}}$ dusp4/16	$k_{\text{synt}} \frac{(\alpha \text{ERK}+\beta \text{JNK})^2}{K_d^2+(\alpha \text{ERK}+\beta \text{JNK})^2}$	k_{deg}dusp4/16	0.5	0.0231	0.0231	1	0	0
$\varnothing \underset{}{\overset{\text{dusp4/16}}{\rightleftharpoons}}$ DUSP4/16	k_{synt}dusp4/16	k_{deg}DUSP4/16	-	0.231	0.0231	-	-	-
$\varnothing \underset{}{\overset{\text{ERK}}{\rightleftharpoons}}$ dusp5/6	$k_{\text{synt}} \frac{(\alpha \text{ERK})^2}{K_d^2+(\alpha \text{ERK})^2}$	k_{deg}dusp5/6	0.5	0.0231	0.0231	0	-	0
$\varnothing \underset{}{\overset{\text{dusp5/6}}{\rightleftharpoons}}$ DUSP5/6	k_{synt}dusp5/6	k_{deg}DUSP5/6	-	0.231	0.0231	-	-	-
$\varnothing \underset{}{\overset{\text{p38}^{**}}{\rightleftharpoons}}$ pp2a	$k_{\text{synt}} \frac{(\alpha \text{p38})^2}{K_d^2+(\alpha \text{p38})^2}$	k_{deg}pp2a	0.5	0.0231	0.0231	0	-	0
$\varnothing \underset{}{\overset{\text{pp2a}}{\rightleftharpoons}}$ PP2A	k_{synt}pp2a	k_{deg}PP2A	-	0.231	0.0231	-	-	-

Table 5: Reactions, rate expressions and parameters of the phosphatase expression proceses in the core model. Units: [a] unitless, [b] min^{-1}. The parameters α, β and γ are structural parameters $\in \{0, 1\}$ that determine which MAPK induces which phosphatase. The values given in the table relate to the core model.

Bagowski, C. P., J. Besser, C. R. Frey, and J. E. Ferrell (2003, Feb). The JNK cascade as a biochemical switch in mammalian cells: ultrasensitive and all-or-none responses. *Curr Biol 13*(4), 315–320.

Bagowski, C. P. and J. E. Ferrell (2001, Aug). Bistability in the JNK cascade. *Curr Biol 11*(15), 1176–1182.

Barthwal, M. K., P. Sathyanarayana, C. N. Kundu, B. Rana, A. Pradeep, C. Sharma, J. R. Woodgett, and A. Rana (2003, Feb). Negative regulation of mixed lineage kinase 3 by protein kinase B/AKT leads to cell survival. *J Biol Chem 278*(6), 3897–3902.

Ben-Levy, R., S. Hooper, R. Wilson, H. F. Paterson, and C. J. Marshall (1998, Sep). Nuclear export of the stress-activated protein kinase p38 mediated by its substrate MAPKAP kinase-2. *Curr Biol 8*(19), 1049–1057.

Bermudez, O., P. Jouandin, J. Rottier, C. Bourcier, G. Pags, and C. Gimond (2011, Jan). Post-transcriptional regulation of the DUSP6/MKP-3 phosphatase by MEK/ERK signaling and hypoxia. *J Cell Physiol 226*(1), 276–284.

Bermudez, O., G. Pags, and C. Gimond (2010, Aug). The dual-specificity MAP kinase phosphatases: critical roles in development and cancer. *Am J Physiol Cell Physiol 299*(2), C189–C202.

Birtwistle, M. R., M. Hatakeyama, N. Yumoto, B. A. Ogunnaike, J. B. Hoek, and B. N. Kholodenko (2007). Ligand-dependent responses of the ErbB signaling network: experimental and modeling analyses. *Mol Syst Biol 3*, 144.

Black, E. J., M. Walker, W. Clark, A. MacLaren, and D. A. F. Gillespie (2002, Sep). Cell transformation by v-jun deactivates ERK MAP kinase signalling. *Oncogene 21*(42), 6540–6548.

Bokemeyer, D., M. Lindemann, and H. J. Kramer (1998, Oct). Regulation of mitogen-activated protein kinase phosphatase-1 in vascular smooth muscle cells. *Hypertension 32*(4), 661–667.

Bokemeyer, D., A. Sorokin, M. Yan, N. G. Ahn, D. J. Templeton, and M. J. Dunn (1996, Jan). Induction of mitogen-activated protein kinase phosphatase 1 by the stress-activated protein kinase signaling pathway but not by extracellular signal-regulated kinase in fibroblasts. *J Biol Chem 271*(2), 639–642.

Borisov, N. M., N. I. Markevich, J. B. Hoek, and B. N. Kholodenko (2005, Aug). Signaling through receptors and scaffolds: independent interactions reduce combinatorial complexity. *Biophys J 89*(2), 951–966.

Borisov, N. M., N. I. Markevich, J. B. Hoek, and B. N. Kholodenko (2006). Trading the micro-world of combinatorial complexity for the macro-world of protein interaction domains. *Biosystems 83*(2-3), 152–166.

Boutros, T., E. Chevet, and P. Metrakos (2008, Sep). Mitogen-activated protein (MAP) kinase/MAP kinase phosphatase regulation: roles in cell growth, death, and cancer. *Pharmacol Rev 60*(3), 261–310.

Brondello, J. M., A. Brunet, J. Pouyssgur, and F. R. McKenzie (1997, Jan). The dual specificity mitogen-activated protein kinase phosphatase-1 and -2 are induced by the p42/p44MAPK cascade. *J Biol Chem 272*(2), 1368–1376.

Cagnol, S. and N. Rivard (2012, Mar). Oncogenic KRAS and BRAF activation of the MEK/ERK signaling pathway promotes expression of dual-specificity phosphatase

4 (DUSP4/MKP2) resulting in nuclear ERK1/2 inhibition. *Oncogene*.

Caunt, C. J. and S. M. Keyse (2012, Jul). Dual-specificity MAP kinase phosphatases (MKPs): shaping the outcome of MAP kinase signalling. *FEBS J Epub ahead of print*.

Chu, Y., P. A. Solski, R. Khosravi-Far, C. J. Der, and K. Kelly (1996, Mar). The mitogen-activated protein kinase phosphatases PAC1, MKP-1, and MKP-2 have unique substrate specificities and reduced activity in vivo toward the ERK2 sevenmaker mutation. *J Biol Chem 271*(11), 6497–6501.

Cirit, M., C.-C. Wang, and J. M. Haugh (2010, Nov). Systematic quantification of negative feedback mechanisms in the extracellular signal-regulated kinase (ERK) signaling network. *J Biol Chem 285*(47), 36736–36744.

Conzelmann, H., D. Fey, and E. D. Gilles (2008). Exact model reduction of combinatorial reaction networks. *BMC Syst Biol 2*, 78.

Dhillon, A. S., S. Hagan, O. Rath, and W. Kolch (2007, May). Map kinase signalling pathways in cancer. *Oncogene 26*(22), 3279–3290.

Dickinson, R. J. and S. M. Keyse (2006, Nov). Diverse physiological functions for dual-specificity MAP kinase phosphatases. *J Cell Sci 119*(Pt 22), 4607–4615.

Douville, E. and J. Downward (1997, Jul). EGF induced SOS phosphorylation in PC12 cells involves P90 RSK-2. *Oncogene 15*(4), 373–383.

Eissing, T., H. Conzelmann, E. D. Gilles, F. Allgwer, E. Bullinger, and P. Scheurich (2004, Aug). Bistability analyses of a caspase activation model for receptor-induced apoptosis. *J Biol Chem 279*(35), 36892–36897.

Frank, T. D., A. M. Carmody, and B. N. Kholodenko (2012). Versatility of cooperative transcriptional activation: a thermodynamical modeling analysis for greater-than-additive and less-than-additive effects. *PLoS One 7*(4), e34439.

Fritsche-Guenther, R., F. Witzel, A. Sieber, R. Herr, N. Schmidt, S. Braun, T. Brummer, C. Sers, and N. Blthgen (2011, May). Strong negative feedback from Erk to Raf confers robustness to MAPK signalling. *Mol Syst Biol 7*, 489.

Fujioka, A., K. Terai, R. E. Itoh, K. Aoki, T. Nakamura, S. Kuroda, E. Nishida, and M. Matsuda (2006, Mar). Dynamics of the Ras/ERK MAPK cascade as monitored by fluorescent probes. *J Biol Chem 281*(13), 8917–8926.

Furuhata, M., E. Takada, T. Noguchi, H. Ichijo, and J. Mizuguchi (2009, Dec). Apoptosis signal-regulating kinase (ASK)-1 mediates apoptosis through activation of JNK1 following engagement of membrane immunoglobulin. *Exp Cell Res 315*(20), 3467–3476.

Gallagher, E. D., S. Xu, C. Moomaw, C. A. Slaughter, and M. H. Cobb (2002, Nov). Binding of JNK/SAPK to MEKK1 is regulated by phosphorylation. *J Biol Chem 277*(48), 45785–45792.

Goldman, E. H., L. Chen, and H. Fu (2004, Mar). Activation of apoptosis signal-regulating kinase 1 by reactive oxygen species through dephosphorylation at serine 967 and 14-3-3 dissociation. *J Biol Chem 279*(11), 10442–10449.

Grethe, S. and M. I. Pörn-Ares (2006, Apr). p38 MAPK regulates phosphorylation of Bad via PP2A-dependent suppression of the MEK1/2-ERK1/2 survival pathway in TNF-alpha induced endothelial apoptosis. *Cell Signal 18*(4), 531–540.

Hanahan, D. and R. A. Weinberg (2011, Mar). Hallmarks of cancer: the next generation. *Cell 144*(5), 646–674.

Hers, I., E. E. Vincent, and J. M. Tavar (2011, Oct). Akt signalling in health and disease. *Cell Signal 23*(10), 1515–1527.

Hu, J.-H., T. Chen, Z.-H. Zhuang, L. Kong, M.-C. Yu, Y. Liu, J.-W. Zang, and B.-X. Ge (2007, Feb). Feedback control of MKP-1 expression by p38. *Cell Signal 19*(2), 393–400.

Huang, C. Y. and J. E. Ferrell (1996, Sep). Ultrasensitivity in the mitogen-activated protein kinase cascade. *Proc Natl Acad Sci U S A 93*(19), 10078–10083.

Iglesias, P. A. and B. P. Ingalls (Eds.) (2009). *Control Theory and Systems Biology*. MIT Press, Cambridge/MA.

Ireton, R., K. Montgomery, R. Bumgarner, R. Samudrala, and J. McDermott (Eds.) (2009). *Computational Systems Biology*, Volume 541 of *Methods in Molecular Biology*. Springer Verlag.

Janssens, V. and J. Goris (2001, Feb). Protein phosphatase 2A: a highly regulated family of serine/threonine phosphatases implicated in cell growth and signalling. *Biochem J 353*(Pt 3), 417–439.

Jeffrey, K. L., T. Brummer, M. S. Rolph, S. M. Liu, N. A. Callejas, R. J. Grumont, C. Gillieron, F. Mackay, S. Grey, M. Camps, C. Rommel, S. D. Gerondakis, and C. R. Mackay (2006, Mar). Positive regulation of immune cell function and inflammatory responses by phosphatase PAC-1. *Nat Immunol 7*(3), 274–283.

Junttila, M. R., S.-P. Li, and J. Westermarck (2008, Apr). Phosphatase-mediated crosstalk between MAPK signaling pathways in the regulation of cell survival. *FASEB J 22*(4), 954–965.

Karlsson, M., J. Mathers, R. J. Dickinson, M. Mandl, and S. M. Keyse (2004, Oct). Both nuclear-cytoplasmic shuttling of the dual specificity phosphatase MKP-3 and its ability to anchor MAP kinase in the cytoplasm are mediated by a conserved nuclear export signal. *J Biol Chem 279*(40), 41882–41891.

Katagiri, C., K. Masuda, T. Urano, K. Yamashita, Y. Araki, K. Kikuchi, and H. Shima (2005, Apr). Phosphorylation of Ser-446 determines stability of MKP-7. *J Biol Chem 280*(15), 14716–14722.

Kholodenko, B. N. (2000, Mar). Negative feedback and ultrasensitivity can bring about oscillations in the mitogen-activated protein kinase cascades. *Eur J Biochem 267*(6), 1583–1588.

Kholodenko, B. N. (2006, Mar). Cell-signalling dynamics in time and space. *Nat Rev Mol Cell Biol 7*(3), 165–176.

Kholodenko, B. N., J. F. Hancock, and W. Kolch (2010, Jun). Signalling ballet in space and time. *Nat Rev Mol Cell Biol 11*(6), 414–426.

Kim, A. H., G. Khursigara, X. Sun, T. F. Franke, and M. V. Chao (2001, Feb). Akt phosphorylates and negatively regulates apoptosis signal-regulating kinase 1. *Mol Cell Biol 21*(3), 893–901.

Kitano, H. (2002, Mar). Systems biology: a brief overview. *Science 295*(5560), 1662–1664.

Kitano, H. (2010). Grand challenges in systems physiology. *Front Physiol 1*, 3.

Kiyatkin, A., E. Aksamitiene, N. I. Markevich, N. M. Borisov, J. B. Hoek, and B. N. Kholodenko (2006, Jul). Scaffolding protein Grb2-associated binder 1 sustains epidermal growth factor-induced mitogenic and survival signaling by multiple positive feedback loops. *J Biol Chem 281*(29), 19925–19938.

Kolch, W. (2005, Nov). Coordinating ERK/MAPK signalling through scaffolds and inhibitors. *Nat Rev Mol Cell Biol 6*(11), 827–837.

Kolch, W., M. Calder, and D. Gilbert (2005, Mar). When kinases meet mathematics: the systems biology of MAPK signalling. *FEBS Lett 579*(8), 1891–1895.

Kucharska, A., L. K. Rushworth, C. Staples, N. A. Morrice, and S. M. Keyse (2009, Dec). Regulation of the inducible nuclear dual-specificity phosphatase DUSP5 by ERK MAPK. *Cell Signal 21*(12), 1794–1805.

Laderoute, K. R., H. L. Mendonca, J. M. Calaoagan, A. M. Knapp, A. J. Giaccia, and P. J. Stork (1999, Apr). Mitogen-activated protein kinase phosphatase-1 (MKP-1) expression is induced by low oxygen conditions found in solid tumor microenvironments. a candidate MKP for the inactivation of hypoxia-inducible stress-activated protein kinase/c-jun N-terminal protein kinase activity. *J Biol Chem 274*(18), 12890–12897.

Lamb, J. A., J.-J. Ventura, P. Hess, R. A. Flavell, and R. J. Davis (2003, Jun). JunD mediates survival signaling by the JNK signal transduction pathway. *Mol Cell 11*(6), 1479–1489.

Legewie, S., H. Herzel, H. V. Westerhoff, and N. Blthgen (2008). Recurrent design patterns in the feedback regulation of the mammalian signalling network. *Mol Syst Biol 4*, 190.

Lemmon, M. A. and J. Schlessinger (2010, Jun). Cell signaling by receptor tyrosine kinases. *Cell 141*(7), 1117–1134.

Lenormand, P., J. M. Brondello, A. Brunet, and J. Pouyssgur (1998, Aug). Growth factor-induced p42/p44 MAPK nuclear translocation and retention requires both MAPK activation and neosynthesis of nuclear anchoring proteins. *J Cell Biol 142*(3), 625–633.

Li, J., M. Gorospe, D. Hutter, J. Barnes, S. M. Keyse, and Y. Liu (2001, Dec). Transcriptional induction of MKP-1 in response to stress is associated with histone H3 phosphorylation-acetylation. *Mol Cell Biol 21*(23), 8213–8224.

Li, S.-P., M. R. Junttila, J. Han, V.-M. Khri, and J. Westermarck (2003, Jul). p38 Mitogen-activated protein kinase pathway suppresses cell survival by inducing dephosphorylation of mitogen-activated protein/extracellular signal-regulated kinase kinase1,2. *Cancer Res 63*(13), 3473–3477.

Lin, S.-C., C.-W. Chien, J.-C. Lee, Y.-C. Yeh, K.-F. Hsu, Y.-Y. Lai, S.-C. Lin, and S.-J. Tsai (2011, May). Suppression of dual-specificity phosphatase-2 by hypoxia increases chemoresistance and malignancy in human cancer cells. *J Clin Invest 121*(5), 1905–1916.

Liu, Q. and P. A. Hofmann (2004, Jun). Protein phosphatase 2A-mediated cross-talk between p38 MAPK and ERK in apoptosis of cardiac myocytes. *Am J Physiol Heart Circ Physiol 286*(6), H2204–H2212.

Mandl, M., D. N. Slack, and S. M. Keyse (2005, Mar). Specific inactivation and nuclear anchoring of extracellular signal-regulated kinase 2 by the inducible dual-specificity protein phosphatase DUSP5. *Mol Cell Biol 25*(5), 1830–1845.

Marshall, C. J. (1995, Jan). Specificity of receptor tyrosine kinase signaling: transient versus sustained extracellular signal-regulated kinase activation. *Cell 80*(2), 179–185.

Masuda, K., H. Shima, M. Watanabe, and K. Kikuchi (2001, Oct). MKP-7, a novel mitogen-activated protein kinase phosphatase, functions as a shuttle protein. *J Biol Chem 276*(42), 39002–39011.

Miller-Jensen, K., K. A. Janes, J. S. Brugge, and D. A. Lauffenburger (2007, Aug). Common effector processing mediates cell-specific responses to stimuli. *Nature 448*(7153), 604–608.

Molton, S. A., D. E. Todd, and S. J. Cook (2003, Jul). Selective activation of the c-Jun N-terminal kinase (JNK)

pathway fails to elicit bax activation or apoptosis unless the phosphoinositide 3'-kinase (PI3K) pathway is inhibited. *Oncogene 22*(30), 4690–4701.

Monick, M. M., L. S. Powers, T. J. Gross, D. M. Flaherty, C. W. Barrett, and G. W. Hunninghake (2006, Aug). Active ERK contributes to protein translation by preventing JNK-dependent inhibition of protein phosphatase 1. *J Immunol 177*(3), 1636–1645.

Nakakuki, T., M. R. Birtwistle, Y. Saeki, N. Yumoto, K. Ide, T. Nagashima, L. Brusch, B. A. Ogunnaike, M. Okada-Hatakeyama, and B. N. Kholodenko (2010, May). Ligand-specific c-Fos expression emerges from the spatiotemporal control of ErbB network dynamics. *Cell 141*(5), 884–896.

Nguyen, L. K., D. Matallanas, D. R. Croucher, A. von Kriegsheim, and B. N. Kholodenko (2012, Feb). Signalling by protein phosphatases and drug development: a systems-centred view. *FEBS J*.

Novak, B. and J. J. Tyson (1993, Dec). Numerical analysis of a comprehensive model of M-phase control in Xenopus oocyte extracts and intact embryos. *J Cell Sci 106 (Pt 4)*, 1153–1168.

Orton, R. J., O. E. Sturm, V. Vyshemirsky, M. Calder, D. R. Gilbert, and W. Kolch (2005, Dec). Computational modelling of the receptor-tyrosine-kinase-activated MAPK pathway. *Biochem J 392*(Pt 2), 249–261.

Park, H.-S., M.-S. Kim, S.-H. Huh, J. Park, J. Chung, S. S. Kang, and E.-J. Choi (2002, Jan). Akt (protein kinase B) negatively regulates SEK1 by means of protein phosphorylation. *J Biol Chem 277*(4), 2573–2578.

Patterson, K. I., T. Brummer, P. M. O'Brien, and R. J. Daly (2009, Mar). Dual-specificity phosphatases: critical regulators with diverse cellular targets. *Biochem J 418*(3), 475–489.

Paumelle, R., D. Tulasne, C. Leroy, J. Coll, B. Vandenbunder, and V. Fafeur (2000, Nov). Sequential activation of ERK and repression of JNK by scatter factor/hepatocyte growth factor in madin-darby canine kidney epithelial cells. *Mol Biol Cell 11*(11), 3751–3763.

Peng, T., T. Zhang, X. Lu, and Q. Feng (2009, Mar). JNK1/c-fos inhibits cardiomyocyte TNF-alpha expression via a negative crosstalk with ERK and p38 MAPK in endotoxaemia. *Cardiovasc Res 81*(4), 733–741.

Phelan, D. R., G. Price, Y. F. Liu, and D. S. Dorow (2001, Apr). Activated JNK phosphorylates the c-terminal domain of MLK2 that is required for MLK2-induced apoptosis. *J Biol Chem 276*(14), 10801–10810.

Plotnikov, A., E. Zehorai, S. Procaccia, and R. Seger (2011, Sep). The MAPK cascades: signaling components, nuclear roles and mechanisms of nuclear translocation. *Biochim Biophys Acta 1813*(9), 1619–1633.

Saez-Rodriguez, J., L. G. Alexopoulos, J. Epperlein, R. Samaga, D. A. Lauffenburger, S. Klamt, and P. K. Sorger (2009). Discrete logic modelling as a means to link protein signalling networks with functional analysis of mammalian signal transduction. *Mol Syst Biol 5*, 331.

Saez-Rodriguez, J., L. G. Alexopoulos, M. Zhang, M. K. Morris, D. A. Lauffenburger, and P. K. Sorger (2011, Aug). Comparing signaling networks between normal and transformed hepatocytes using discrete logical models. *Cancer Res 71*(16), 5400–5411.

Saitoh, M., H. Nishitoh, M. Fujii, K. Takeda, K. Tobiume, Y. Sawada, M. Kawabata, K. Miyazono, and H. Ichijo (1998, May). Mammalian thioredoxin is a direct inhibitor of apoptosis signal-regulating kinase (ASK) 1. *EMBO J 17*(9), 2596–2606.

Sakon, S., X. Xue, M. Takekawa, T. Sasazuki, T. Okazaki, Y. Kojima, J.-H. Piao, H. Yagita, K. Okumura, T. Doi, and H. Nakano (2003, Aug). NF-kappaB inhibits TNF-induced accumulation of ROS that mediate prolonged MAPK activation and necrotic cell death. *EMBO J 22*(15), 3898–3909.

Santos, S. D. M., P. J. Verveer, and P. I. H. Bastiaens (2007, Mar). Growth factor-induced MAPK network topology shapes ERK response determining PC-12 cell fate. *Nat Cell Biol 9*(3), 324–330.

Schachter, K. A., Y. Du, A. Lin, and K. A. Gallo (2006, Jul). Dynamic positive feedback phosphorylation of mixed lineage kinase 3 by JNK reversibly regulates its distribution to Triton-soluble domains. *J Biol Chem 281*(28), 19134–19144.

Shen, H. and Z. Liu (2006, Mar). JNK signaling pathway is a key modulator in cell death mediated by reactive oxygen and nitrogen species. *Free Radic Biol Med 40*(6), 928–939.

Shen, Y. H., J. Godlewski, J. Zhu, P. Sathyanarayana, V. Leaner, M. J. Birrer, A. Rana, and G. Tzivion (2003, Jul). Cross-talk between JNK/SAPK and ERK/MAPK pathways: sustained activation of JNK blocks ERK activation by mitogenic factors. *J Biol Chem 278*(29), 26715–26721.

Small, G. W., Y. Y. Shi, L. S. Higgins, and R. Z. Orlowski (2007, May). Mitogen-activated protein kinase phosphatase-1 is a mediator of breast cancer chemoresistance. *Cancer Res 67*(9), 4459–4466.

Snchez-Prez, I., M. Martnez-Gomariz, D. Williams, S. M. Keyse, and R. Perona (2000, Oct). CL100/MKP-1 modulates JNK activation and apoptosis in response to cisplatin. *Oncogene 19*(45), 5142–5152.

Stepniak, E., R. Ricci, R. Eferl, G. Sumara, I. Sumara, M. Rath, L. Hui, and E. F. Wagner (2006, Aug). c-jun/AP-1 controls liver regeneration by repressing p53/p21 and p38 MAPK activity. *Genes Dev 20*(16), 2306–2314.

Sturm, O. E., R. Orton, J. Grindlay, M. Birtwistle, V. Vyshemirsky, D. Gilbert, M. Calder, A. Pitt, B. Kholodenko, and W. Kolch (2010). The mammalian MAPK/ERK pathway exhibits properties of a negative feedback amplifier. *Sci Signal 3*(153), ra90.

Sundaramurthy, P. and S. Gakkhar (2010, Dec). Dynamic modeling and simulation of JNK and p38 kinase cascades with feedbacks and crosstalks. *IEEE Trans Nanobioscience 9*(4), 225–231.

Sundaramurthy, P., S. Gakkhar, and R. Sowdhamini (2009). Computational prediction and analysis of impact of the cross-talks between JNK and p38 kinase cascades. *Bioinformation 3*(6), 250–254.

Ventura, J.-J., P. Cogswell, R. A. Flavell, A. S. Baldwin, and R. J. Davis (2004, Dec). JNK potentiates TNF-stimulated necrosis by increasing the production of cytotoxic reactive oxygen species. *Genes Dev 18*(23), 2905–2915.

Ventura, J.-J., A. Hbner, C. Zhang, R. A. Flavell, K. M. Shokat, and R. J. Davis (2006, Mar). Chemical genetic analysis of the time course of signal transduction by JNK. *Mol Cell 21*(5), 701–710.

von Kriegsheim, A., D. Baiocchi, M. Birtwistle, D. Sumpton, W. Bienvenut, N. Morrice, K. Yamada, A. Lamond, G. Kalna, R. Orton, D. Gilbert, and W. Kolch (2009, Dec). Cell fate decisions are specified by the dynamic ERK interactome. *Nat Cell Biol 11*(12), 1458–1464.

Wagner, E. F. and A. R. Nebreda (2009, Aug). Signal integration by JNK and p38 MAPK pathways in cancer development. *Nat Rev Cancer 9*(8), 537–549.

Wang, Z., J.-Y. Zhou, D. Kanakapalli, S. Buck, G. S. Wu, and Y. Ravindranath (2008, Dec). High level of mitogen-activated protein kinase phosphatase-1 expression is associated with cisplatin resistance in osteosarcoma. *Pediatr Blood Cancer 51*(6), 754–759.

Westermarck, J., S. P. Li, T. Kallunki, J. Han, and V. M. Khri (2001, Apr). p38 mitogen-activated protein kinase-dependent activation of protein phosphatases 1 and 2A inhibits MEK1 and MEK2 activity and collagenase 1 (MMP-1) gene expression. *Mol Cell Biol 21*(7), 2373–2383.

Wong, H. R., K. E. Dunsmore, K. Page, and T. P. Shanley (2005, Nov). Heat shock-mediated regulation of MKP-1. *Am J Physiol Cell Physiol 289*(5), C1152–C1158.

Xiong, W. and J. E. Ferrell (2003, Nov). A positive-feedback-based bistable 'memory module' that governs a cell fate decision. *Nature 426*(6965), 460–465.

Xu, S. and M. H. Cobb (1997, Dec). MEKK1 binds directly to the c-jun N-terminal kinases/stress-activated protein kinases. *J Biol Chem 272*(51), 32056–32060.

Yin, Y., Y.-X. Liu, Y. J. Jin, E. J. Hall, and J. C. Barrett (2003, Apr). PAC1 phosphatase is a transcription target of p53 in signalling apoptosis and growth suppression. *Nature 422*(6931), 527–531.